CHAPTER III

Anion sensory studies of amide ferrocene calix[4]arene derivatives

3.1 Introduction

Anion recognition is an area of interest in the field of biological systems[60], environmental pollutants[61] and chemical processes. Recently, anion chemical sensors play important roles in fundamental principles of supramolecular chemistry. Artificial molecules were constructed in the part of anion binding site linking to the sensory unit. Generally, designed sensory molecules contain functional groups that have the capacity for hydrogen bonding and electrostatic interactions as well as the sensory units that can gives electrochemical or optical signals.

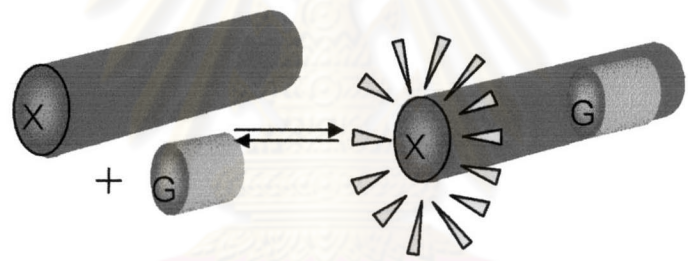

G = Cationic, anionic and Neutral; X = Receptor or signaling Group (Redox / Photo-active)

Figure 3.1.1 Depict of concept of electrochemical/optical recognition[62]

Moreover, ditopic receptors have been focused on studying simultaneous cation and anion recognition. Most of them were designed in order to enhance the binding ability using ion pair interactions. Many molecules employed calix[4]arene framework as a building blockin order to augment the binding ability caused by the rigid and preorganized molecule. Calix[4]arene is a popular building block because it can be derivatized on both lower and upper rims. For instance, Ungaro and coworkers[63] reported calix[4]arene-based heteroditopic receptors having the cation binding site of tetraamide on the lower rim and the anion binding site of monothiourea on the upper rim. (**Figure 3.1.2**)

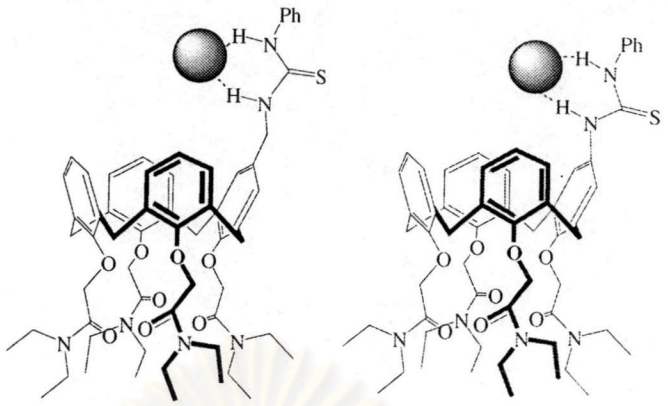

3.1 3.2

Figure 3.1.2 The heteroditopic receptors **3.1** and **3.2**

The tetraamide group on the lower rim binds Na^+ selectively. Association constants of ligand **3.2** in the presence of Na^+ on the tetraamide group have higher value than those of **3.1** in the absence of Na^+ because the complexes of Na^+ at tetraamide give the influence of electron-withdrawing on NH group directly. In contrast, the complexes of ligand **3.2** in the presence of Na^+. Ligand **3.1** has a CH_2 spacer between the aromatic part and the thiourea unit. This spacer prevents the electron-withdrawing effect toward NH proton resulting in no change of anion binding properties compared to the free ligand. Both ligands bind cation and anions simultaneously using the enhancement of binding ability via ion pair interaction. Nevertheless, the heteroditopic calix[4]arene receptors bearing the cationic and anionic binding sites on the same side were synthesized to enhance the binding ability using ion pair interaction. Beer and coworkers[64] designed the heteroditopic rhenium (I) and ruthenium (II) bipyridyl calix[4]arene receptors to bind both cationic and anionic species. (**Figure 3.1.3**)

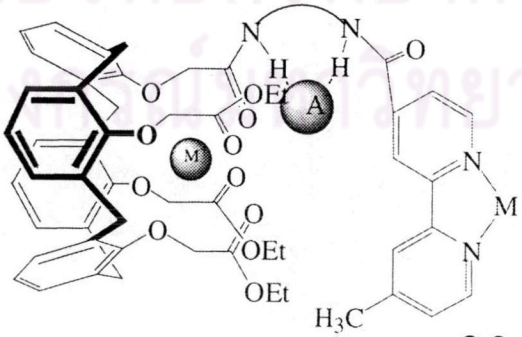

3.3

M = $Re(CO)_3$, $(bipy)_2Ru^{2+}(PF_6^-)_2$

Figure 3.1.3 The heteroditopic receptors based on calix[4]arene

They reported that these ligands bind Li^+ and Na^+ strongly at ethyl ester groups. Moreover, the anion affinity in the presence of lithium and sodium cations was enhanced in case of bromide and iodide, possibly via ion pair interactions. However, the stability constants show higher values in the presence of Na^+.

Jurczak and coworkers have developed an amide-based macrocyclic sensor for

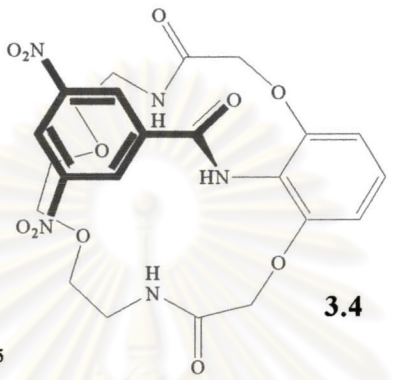

3.4

anions.[65]

Figure 3.1.4 Anion sensory receptor based on an amide group

Figgure 3.1.5 Colour changes induced by the addition of anions. From left to right (in acetonitrile) Ligand, **L**+F^-, **L**+Cl^-, **L**+Br^-, **L**+AcO^-, **L**+$H_2PO_4^-$, **L**+HSO_4^-.

They found that the ligand shown in **Figure 3.14** bind all anionic species in the stoichiometry of 1:1 for host: guest except F^- (1:2 ratio) in either CH_3CN or DMSO. The stability constants of this ligand and anion indicated high binding affinity for anions in CH_3CN. Additionally, color of the solution changes obviously when the ligand bind F^-, AcO^- and $H_2PO_4^-$. This molecule is thus an excellent colorimetric detector for anions because the different color displays upon addition of various anions (F^-, AcO^- and $H_2PO_4^-$) as shown in **Figure 3.1.5**

Many researchers have synthesized anion sensor based on metallocenes which can act as electrochemical sensory devices. In particular, the immobilisation of redox-responsive receptor systems on electrode surfaces.[66-68] In 2002,[69] Barrio and coworkers prepared an

anion sensor based on a pyrrole-cobaltocenium receptor (**3.5**, **Figure 3.1.6**) and studied the electrochemical recognition of anions such as $H_2PO_4^-$, HSO_4^-, Cl^- and Br^-. Electrochemical properties of complexes of ligand and anions in solution and in immobilization on electrode are different. It was found that the electrochemical recognition of anions on the modified electrode showed larger cathodic shift than those of anions in solution and this receptor prefers to bind $H_2PO_4^-$ in both systems.

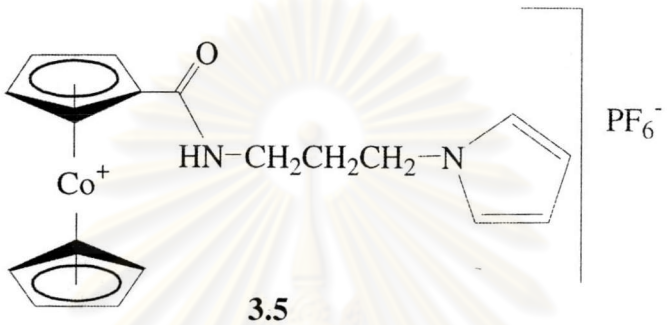

3.5

Figure 3.1.6 The pyrrole-cobaltocenium receptor for electrochemical recognition of anions

Ferrocene units for anionic and cation recognition have been well-known because the ferrocene unit exhibits good electrochemical signals by means of reversible processes. Additionally, the cyclopentadiene ring is easy to be derivetized. These types of compounds can also be used as electrochemical sensor. In 1999, Beer et al.[70] reported the anion recognition of upper-rim cobaltocenium calix[4]arene receptors and found that they formed complexes with carboxylate anions, dihydrogen phosphate and halide anions to a different extent. Recently, ion-pair recognition has been recognized by supramolecular chemists. It is due to its potential applications in metal ion and anion attraction or metal-controlled anion sensing devices.[71] In this dissertation, we synthesized the calix[4]arene derivatives having the amide ferrocene at the upper rim and ethylester at the lower rim for anion and cation recognition, respectively. We also studied electrochemical properties of the synthesized compounds before and after addition of anions.

3.2. Experimental section

3.2.1 Synthesis of Calix[4]arene Derivatives

3.2.1.1 General Procedure

3.2.1.1.1 Analytical Measurment

Nuclear Magnetic Resonance (NMR) spectra were recorded on Bruker ACF 200 MHz and 400 MHz as well as JMN (Jeol) 500 MHz spectrometer. All chemical shifts were reported in part per million (ppm) using the residual proton or cabon signal in deuterated solvents as internal references. Each proton was assigned by 2D NMR techniques such as ^{1}H-^{1}H-COSY and ^{1}H-^{13}C-HMQC. Assignments of ^{13}C-NMR spectra were carried out by DEPT-90 and DEPT-135.

Elemental analyses were carried out on a Perkin-Elmer CHON/S analyzer (PE 2400 series II) by ignition combustion gas chromatography separated by frontal analyses and quantitatively detected by thermal conductivity detector. All melting points were obtained on an Electrothermal 9100 apparatus and uncorrected. Mass spectrometer results were recorded on Micromass LCT Electrospray Time of Flight Mass Spectrometer.

X-Ray data was collected on Enraf Nonius KappaCCD area detector diffractometer (ϕ scans and ω scans to fill *Ewald* sphere) using monochromatised Mo-Kα radiation. Data collection and cell refinement were carried out by Denzo.[72] Absorption correction was applied by SORTAV.[73-74] The structure were solved and refined by full-matrix least-square on F2 using the computer program SHELXS97.[75]

3.2.1.1.2 Materials

Unless otherwise noted, all materails and solvents were standard analytical grade, purchased from Fluka, BDH, Aldrich, Carlo Erba, Merck, J. T. Baker or Lab scan. They were used without further purification. Commercial grade solvents such as acetone, dichloromethane, hexane, methanol and ethyl acetate were purified by distillation. Acetonitrile and toluene were dried over CaH_2 and freshly distilled under nitrogen prior to used. DMF was dried with CaH_2, distilled under reduced pressure and stored over

molecular sieves 3 Å or 4 Å under N_2. Standrad Schlenk line technique was employed for all experiments. Column chromatographic operations were carried out on silica gel (Kieselgel 60, 0.063-0.200 nm, Merck). Thin-layer chromatography (TLC) were performed on silica gel plates (Kieselgel 60 F_{254}, 1 mm, Merck), *p-tert*-butylcalix[4]arene and calix[4]arene were was prepared according to published procedures.[76]

3.2.1.2 Experimental procedure

3.2.1.2.1 Prepatration of 26, 28-dimethoxycalix[4]arene (1a)[77]

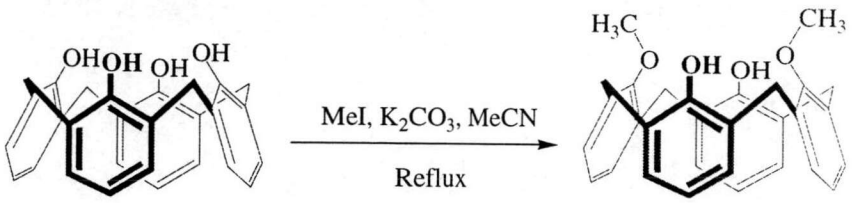

1a

Calix[4]arene (0.425 g, 1.0 mmol) and K_2CO_3 (0.1512 g, 1.09 mmol) was suspended in CH_3CN (10 mL) and the mixture was stirred at room temperature for 1 h. Iodomethane (0.1313 g, 2.20 mmol) was then added and the mixture was heated at reflux overnight. The mixture was cooled to room temperature. The reaction was filtered to take K_2CO_3 off and then the filtrate was concentrated by a rotary evaporator. The residue was dissolved in dichloromethane and washed with 3 M HCl 3 times. The organic layer was dried over anhydrous $NaSO_4$. The volumn of the solvent was reduced by using a rotary evaporator. Upon adding CH_3OH, a white solid of compound **1a** precipitated (0.397 g, 87.77% yield).

Characterization data for 1a

^{1}H-NMR spectrum (200 MHz, $CDCl_3$): δ(in ppm)

δ 7.72 (s, 2H, O*H*), 7.09-6.63 (m, 12H, Ar*H*), 4.33 and 3.42 (d, *J* = 13.2 Hz, 8H, ArCH_2Ar), 3.97 (s, 6H, OCH_3).

3.2.1.2.2 Preparation of 26,28-dimethylethylestercalix[4]arene (1b)

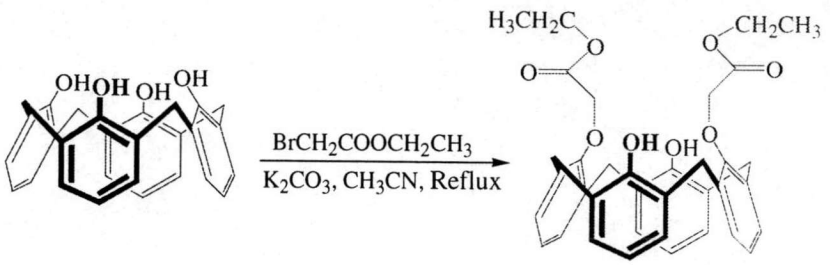

1b

Calix[4]arene (1.0 g, 2.36 mmol) and K_2CO_3 (2.50 g, 23.6 mmol) was suspended in CH_3CN (15 mL) and the mixture was stirred at room temperature for 1 h. Bromoethyl acetate (0.87 g, 5.20 mmol) was then added and the mixture was heated at reflux for 4 h. The mixture was cooled to room temperature. The reaction was filtered to take K_2CO_3 off and then the filtrate was concentrated by rotary evaporator. The residue was dissolved in dichloromethane and washed with saturated NH_4Cl 3 times. The organic layer was dried over anhydrous $NaSO_4$. The volumn of the solvent was reduced by using a rotary evaporator. Upon adding CH_3OH, a white solid of **1b** was obtained (0.801g, 57%).

Characterization data for 1b

^{1}H-NMR spectrum (200 MHz, $CDCl_3$): δ (in ppm)

δ 7.57 (s, 2H, O*H*), 7.04 (d, *J* = 7.47 Hz, 4H, *m*-Ar*H*OR), 6.89 (d, *J* = 7.41 Hz, 4H, *m*-Ar*H*OH), 6.76-6.60 (m, 4H, *p*-Ar*H*OR and *p*-Ar*H*OH), 4.71 (s, 4H, ArOCH_2-), 4.46 and 3.38 (dd, *J* = 13.3, ArCH_2Ar), 4.37-4.27 (q, *J* = 7.23 Hz, -OCH_2CH$_3$), 1.34 (t, *J* = 6.53 Hz, 6H, -OCH$_2$CH_3)

Melting point: 180 °C

3.2.1.2.3 Preparation of 5,7-dinitro-26,28-dimethoxycalix[4]arene (2a)

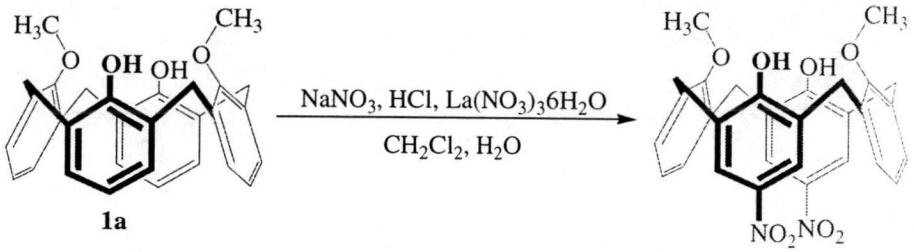

1a **2a**

To a solution (CH_2Cl_2, 494 mL) of 26,28-dimethoxycalix[4]arene (**1a**) (10 g, 22.1 mmol) was added $NaNO_3$ (5.64 g ; 66.3 mmol) and a catalytic amount of $La(NO_3)_3.6H_2O$ in a mixture of H_2O (304 mL) and concentrated HCl (55 mL). The mixture was stirred overnight at room temperature. The colour of the mixture turned yellow. The aqueous layers were then separated and extracted with CH_2Cl_2 (250x2). The organic layer was combined and washed with saturated aqueous NH_4Cl (250x2) and dried over anhydrous Na_2SO_4. The solvent was removed by a rotary evaporator and the product was crytallized by adding hexane to give a white solid (8.51 g, 71% yield). mp > 320 ^{o}C decomposed.

Characterization data for 2a

^{1}H-NMR spectrum (200 MHz, $CDCl_3$): δ (in ppm)

δ 8.93(s, 2H, -O*H*), 8.04 (s, 4H, *H*Ar-NO_2), 6.94 (d, 4H, *m*-*H*Ar-OCH_3, J = 7.2 Hz), 6.85-6.77 (t, 2H, *p*-*H*Ar-OCH_3, J = 7.4), 4.28 and 3.52 (dd, 8H, *H*AB system, J = 13.3 Hz), 4.02 (s, 6H, -OCH_3).

Melting point: >320 ^{o}C decomposed

3.2.1.2.4 Preparation of 5,7-dinitro-26,28-dimethylethylestercalix[4]arene (2b)

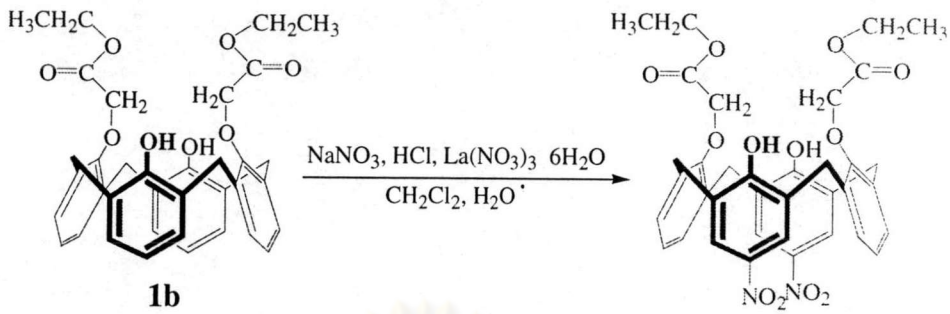

1b **2b**

To a solution (CH_2Cl_2, 140 mL) of 26,28-dimethylethylestercalix[4]arene (**1b**) (3.15 g, 5.26 mmol) was added $NaNO_3$ (2.70 g, 31.74 mmol) and a catalytic amount of La $(NO_3)_3.6H_2O$ in a mixture of H_2O (88 mL) and concentrated HCl (14.3 mL). The mixture was stirred overnight at room temperature and then worked up in a similar fashion as **2a** to give a yellow solid **2b** (3.17 g, 88% yield).

Characterization data for 2b

^{1}H-NMR spectrum (200 MHz, $CDCl_3$): δ (in ppm)

δ 8.90 (s, 2H, -O*H*), 8.01 (s, 4H, *O*-Ar*H*-NO_2), 6.91 (d, *J* = 8.34 Hz, *m*-Ar*H*-OH), 6.84 (t, *J* = 6.44 Hz, 2H, *p*-Ar*H*-OR), 4.67 (s, 4H, OCH_2CO), 4.45, and 3.49 (dd, *J* = 13.32 Hz, 8H, AB system), 4.35 (q, *J* = 7.14 Hz, 4H, OCH_2CH_3), 1.39 (t, *J* = 8.7 Hz, 6H, -CH_2CH_3)

Melting point : 250 °C

3.2.1.2.5 Preparation of 5,7-dinitro-25,26,27,28-tetramethoxycalix[4]arene (3a)

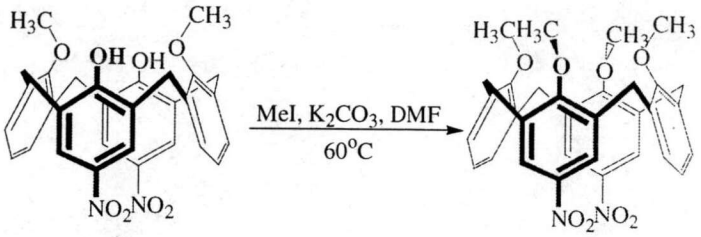

2a **3a**

A solution (DMF, 10 mL) of 5,7-dinitro-26,28-dimethoxycalix[4]arene (**2a**) (0.2713 g, 0.5 mmol) and K_2CO_3 (0.695 g, 5 mmol) was stirred at room temperature for 1 h. CH_3I (0.50 mL, 8.00 mmol) was then added and the mixture was heated at 60 °C for 7 days. After the mixture was cooled to room temperature, the solvent was removed under reduced pressure. The residue was dissolved in CH_2Cl_2 (30 mL) and washed with water and brine (2x30 mL) and then dried over anhydrous Na_2SO_4. The solvent was removed by using a rotary evaporator. Upon addition of CH_3OH, a white solid **3a** precipitated (0.203g.;71% yield).

Characterization data for 3a

^{1}H-NMR spectrum (200 MHz, $CDCl_3$): δ (in ppm)

δ 8.19-6.43 (m, 10H, Ar*H*), 4.37, 4.05, 3.28 and 3.17 (d, each *J* = 13.3 Hz, 8H, ArCH_2Ar), 3.85-3.72 (m, 12H, -OCH_3).

ESI-TOF mass spectrum: $C_{32}H_{30}N_2O_8$ = 571.30 ([M+H$^+$]) m/z.

Melting point: 260 °C

3.2.1.2.6 5,7-dinitro-25,26,27,28-dimethoxydimethylethylestercalix[4]arene (3b)

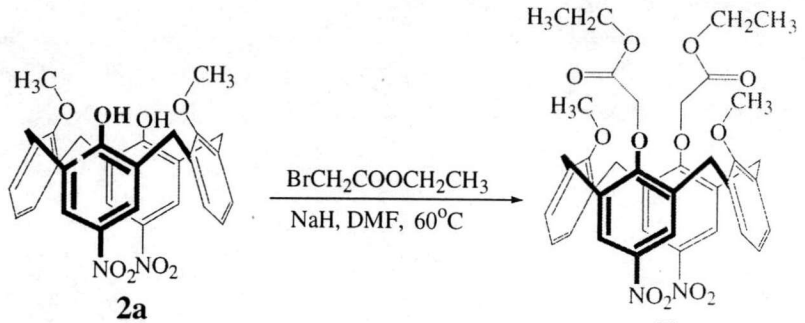

2a **3b**

A solution (DMF, 20 mL) of 5,7-dinitro-26,28-dimethoxy dimethylethyl ester calix[4]arene (**2a**) (0.543 g, 1.0 mmol) and NaH (0.12 g, 5.0 mmol) was stirred at room temperature for 1 h. Bromoethyl acetate (0.40 mL, 3.0 mmol) was then added and the mixture was heated at 60 °C overnight. The reaction was worked up corresponding to the procedure for **3a** to provide a pale yellow solid **3b** (0.436g, 61%).

Characterization data for 3b

^{1}H-NMR spectrum (200 MHz, $CDCl_3$): δ (in ppm)

δ 7.83-7.08 (m, 10H, *H*-Aromatic), 4.45 (s, 4H, -OC*H*$_2$CO-), 4.32-4.21 (q, 4H, -OC*H*$_2$CH$_3$, *J* = 7.2 Hz), 3.96-2.99 (m, 14H, -OC*H*$_3$ and *H*AB system), 1.34-1.27 (td, 6H, -CH$_2$C*H*$_3$, *J* = 7.1 and 1.5 Hz).

Elemental Analysis:

Anal. Calcd for $C_{38}H_{38}O_{12}N_2$: C, 63.86 ; H, 5.36 ; N, 3.92

Found : C, 63.85 ; H, 5.29 ; N, 3.88

3.2.1.2.7 Preparation of 5,7-dinitro-25,26,27,28-dimethylethylestercalix[4]arene (3c)

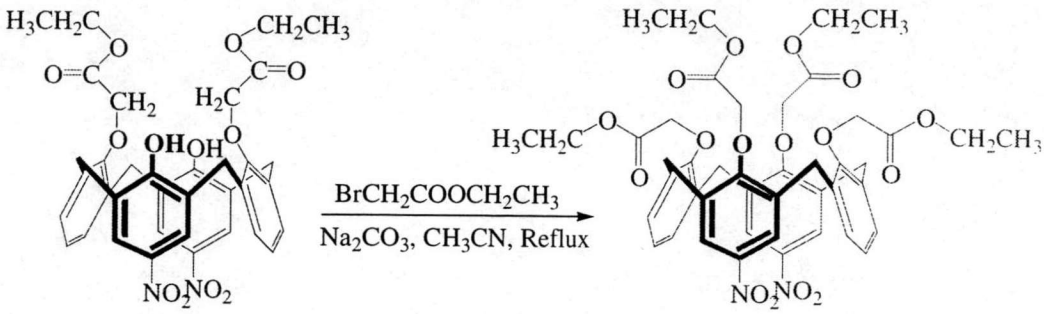

2b **3c**

A solution (CH_3CN, 30 mL) of 5,7-dinitro-26,28-dimethylethylestercalix[4]arene (**2b**) (0.60 g, 1.0 mmol) and Na_2CO_3 (1.14 g, 10.4 mmol) was stirred at room temperature for 1 h. Bromoethyl acetate (1.20 mL, 1.67 mmol) was then added and the mixture was refluxed overnight. The mixture was allowed to cool to room temperature and Na_2CO_3 was removed by filtration. The mixture was evaporated using a rotary evaporator. The residue was dissolved in CH_2Cl_2 (20 mL). The organic phase was then washed with saturated NH_4Cl 3 times. The organic layer was dried over anhydrous Na_2SO_4. The solvent was removed under reduced pressure. Finally, compound **3c** precipitated as a yellow solid upon addition of CH_3OH (0.524 g, 61%).

Characterization data for 3c

^{1}H-NMR spectrum (200 MHz, $CDCl_3$): δ (in ppm)

δ 8.90 (s, 2H, O*H*), 8.01 (s, 4H, *m*-Ar*H*OH), 6.99 (d, *J* = 6.97 Hz, *m*-Ar*H*OR), 6.89-6.80 (m, 2H, *p*-Ar*H*OR), 4.71 (s, 4H, -OCH_2CO-), 4.45 and 3.49 (dd, *J* = 13.3 Hz, 8H, ArCH_2Ar), 4.40-4.29 (q, *J* = 7.17 Hz, -OCH_2CH$_3$), 1.35 (t, *J* = 7.13 Hz, 6H, OCH$_2$CH_3)

Melting point: 190 °C

3.2.1.2.8 Preparation of 5,7-diamino-25,26,27,28-tetramethoxycalix[4]arene (4a)

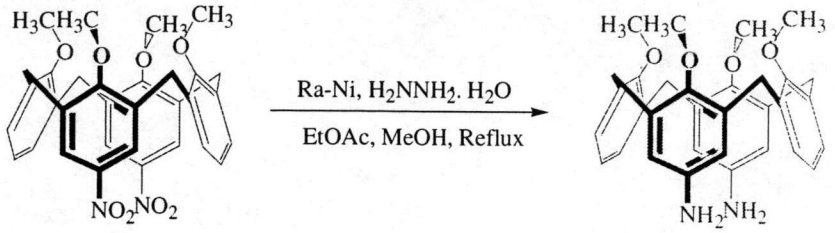

3a **4a**

5,7-Dinitro-25,26,27,28-tetramethoxycalix[4]arene (1.3928 g, 1.95 mmol) and Raney Ni (2.0951 g) were suspended in the mixture of ethylacetate (80 mL) and CH_3OH (40 mL). Hydrazine (4 mL) was then added into the mixture. The mixture was refluxed for 2 h. and allowed to cool to room temperature. The solvent was subsequently removed under reduced pressure. The residue was dissolved in CH_2Cl_2 and extracted and washed with several portions of H_2O. The organic layer was separated, combined and dried over anhydrous Na_2SO_4. The solvent was removed under reduced pressure to give a pale-white solid **4a** (0.976 g, 98% yield).

Characterization data for 4a

^{1}H-NMR spectrum (200 MHz, $CDCl_3$): δ (in ppm)

δ 7.04-6.43 (m-br, 6H, Ar*H*), 6.09 (s, br, 4H, *o*-Ar*H*-NH_2), 4.26-2.91 (m, br, 20H, OCH_3 and AB system).

ES-TOF mass spectrum: $C_{32}H_{34}N_2O_4$ = 511.30 ([M+H^+]) m/z.

3.2.1.2.9 Preparation of 5,7-diamino-25,26,27,28-dimethoxy dimethylethyl ester calix[4]arene (4b)

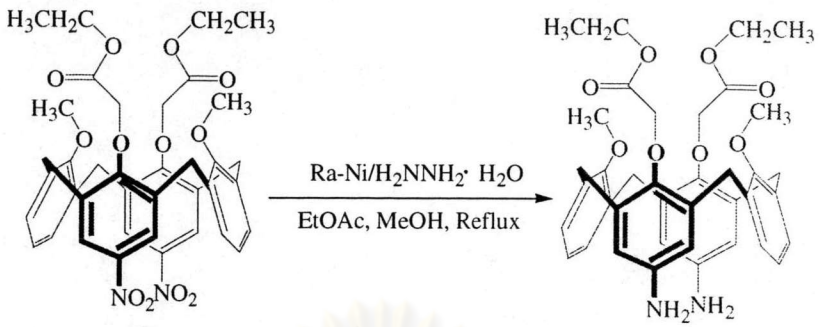

3b **4b**

5,7-Dinitro-25,26,27,28-dimethoxydimethylethylestercalix[4]arene (**3b**) (0.714 g, 1.0 mmol) and Raney Ni (1.0 g) were suspended in the mixture of ethylacetate (38 mL) and CH_3OH (28 mL). Hydrazine (4 mL) was subsequently added. The mixture was refluxed for 2 h and allowed to cool to room temperature. The reaction was worked up as described previously (**4a**). Compound **4b** was obtained as a white solid (0.628 g, 96%).

Characterization data for 4b

^{1}H-NMR spectrum (200 MHz, $CDCl_3$): δ (in ppm)

δ 7.22 (d, 4H, *m*-*H*Ar-OCH_3, J = 6.9 Hz), 6.93-6.86 (t, 2H, *p*-*H*Ar-OCH_3, J = 7.2 Hz), 5.69 (s, 4H, *o*-*H*Ar-NH_2), 4.40 (d, 4H, AB system, J = 13.1 Hz and s, 4H, *o*-CH_2CO-), 4.30-4.20 (q, 4H, -O$CH_2$$CH_3$, J = 7.1 Hz), 3.96 and 3.46 (s, 6H, -OCH_3), 3.10 (d, 4H, AB system, J = 12.8 Hz), 1.33-1.26 (t, 6H,-O$CH_2$$CH_3$, J = 7.1 Hz).

ESI-TOF mass spectrum: $C_{38}H_{42}N_2O_8$ = 655.70 ([M+H$^+$]) m/z.

Elemental Analysis:

Anal. Calcd.for $C_{38}H_{42}N_2O_8$: C, 69.71 ; H, 6.47 ; N, 4.28
Found : C, 69.71 ; H, 6.25 ; N, 4.26.

3.2.1.2.10 Preparation of 5,7-diamino-25,26,27,28-tetramethylethylestercalix[4] arene (4c)

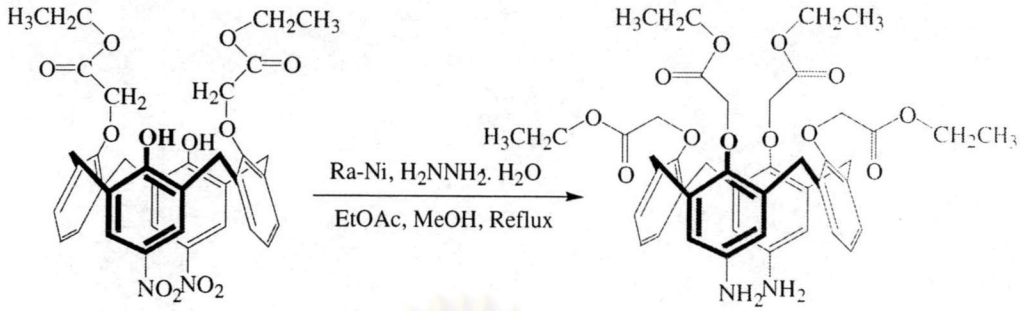

3c **4c**

5,7-Dinitro-25,26,27,28-tetramethylethylestercalix[4]arene (1.47 g, 1.52 mmol) (**3c**) and Raney Ni (1.52 g) were suspended in the mixture of ethylacetate (58 mL) and CH_3OH (42 mL). Hydrazine (6 mL) was subsequently added. The mixture was refluxed for 2 h. and allowed to cool to room temperature. The reaction was worked up as described previously (**4a**). Compound **4c** was obtained as a white solid (1.15g, 95%).

Characterization data for 4c

^{1}H-NMR spectrum (200 MHz, $CDCl_3$): δ (in ppm)

δ 6.69-6.59 (m, 6H, m-Ar*H*-OR), 6.01 (s, 4H, *o*-Ar*H*-NH_2), 4.78 and 3.10 (d, J = 13.1 Hz, 8H, AB system), 4.70 (s, 4H, ArOCH_2-), 4.61 (s, 4H, NH_2-Ar-OCH_2-), 4.18 (q, J = 7.1 Hz, 8H, *o*-CH_2CH$_3$), 1.26 (t, J = 7.2 Hz, 12 H, -CH_3)

ESI-TOF mass spectrum: $C_{44}H_{50}N_2O_{12}$ = 799.13 ([M+H$^+$]) m/z.

3.2.1.2.11 Preparation of 5,7-diamideferrocenyl-25,26,27,28-tetramethoxycalix [4]arene (5a)

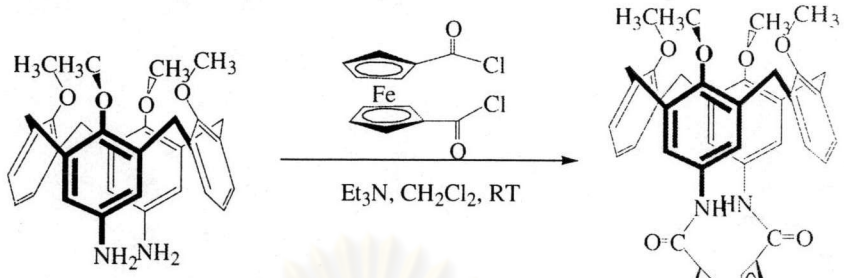

4a **5a**

Into a two-necked round-bottomed flask, the mixture of tetramethoxy-diaminocalix[4]arene (**4a**) (0.786 g, 1.54 mmol) and triethylamine (0.5 mL) in dichloromethane (30 mL) was stirred at room temperature under N_2. 1,1-Bis (chlorocabonyl)ferrocene (0.6201g, 2.0 mmol) in dichloromethane (30 mL) was transferred into the mixture via cannula. The mixture was stirred at room temperature under N_2 for 4 h. It was then washed with several portions of H_2O. The organic layer was dried with anhydrous $NaSO_4$. The solvent was removed under reduced pressure to afford a dark red residue which was then placed on a silica gel chromotography column. Compound **5a** was eluted from the column using 10% EtOAc in CH_2Cl_2 as eluant. Compound **5a** is an orange solid (0.576 g., 50%). Orange crystals pf **5a** were obtained by slow diffusion of hexane into CH_2Cl_2 and CH_3OH solution of compound **5a**.

Characterization data for 5a

^{1}H-NMR spectrum (500 MHz, d^6-Acetone): δ (in ppm)

δ 8.09 (s, 2H, -N*H*-(pc)), 7.86 (s, 2H,-N*H*-(c)), 7.59 and 6.46 (d, *J* =3 Hz, 4H, -Ar*H*-NH-(pc)), 7.22 (d, *J* = 8 Hz, 4H, *m*-Ar*H* (c)) 7.18 and 7.10 (d, *J* = 7.5 Hz, 4H, *m*-Ar*H*, (pc)), 7.01 (t, *J* = 7.5 Hz, 2H, *p*-Ar*H* (c)), 6.93 and 6.81 (t, *J* = 7.5 Hz, 2H, *p*-Ar*H* (pc)), 6.47 (s, 4H, -NH-Ar*H*- (c)) 5.00 and 4.83 (m, 4H, *o*-Cp*H* (pc)), 4.75 (t, *J* = 2.5 Hz, 4H, *o*-Cp*H* (c)), 4.41 and 4.36 (m, 4H, m-Cp*H* (pc)), 4.36 and 3.14 (d, *J* =13.5, 8H, AB system(c)), 4.313 (t, *J* = 2 Hz, 4H-Cp*H* (c)), 4.04 and 3.06 (d, *J* = 14 Hz, 8H, AB system), 3.92-3.65 (m, 21H, -OC*H*$_3$ (pc and c)), 2.86 (s, 3H, -OC*H*$_3$ (pc)).

ESI-TOF mass spectrum: $C_{44}H_{40}N_2O_6Fe$ = 749.50 ([M+H$^+$]) m/z.

Elemental Analysis:

Anal. Calcd. for $C_{44}H_{40}N_2O_6Fe \cdot 0.5\ CH_2Cl_2$: C, 67.56; H, 5.22; N, 3.45.
Found : C, 67.72; H, 5.24; N, 3.55.

Melting point: 200 °C decomposed

3.2.1.2.12 Preparation of 5,7-diamideferrocenyl-25,26,27,28-dimethoxy dimethylethylestercalix[4] arene (5b)

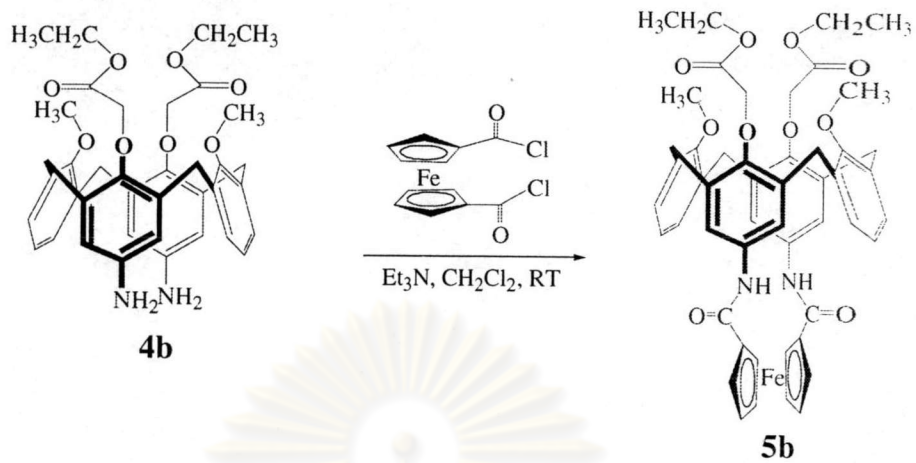

4b **5b**

Into a two-necked round-bottomed flask, the mixture of dimethoxy dimethyl ethylester-diaminocalix[4]arene(**4b**) (1.31 g, 2.0 mmol) and triethylamine (1.0 mL) in dichloromethane (40 mL) was stirred at room temperature under N_2. 1,1-Bis (chlorocabonyl)ferrocene (0.620 g, 2.1 mmol) in dichloromethane (20 mL) was transferred into the mixture via cannula. The mixture was stirred at room temperature under N_2 for 4 h. It was then washed with several portions of H_2O. The organic layer was dried with anhydrous $NaSO_4$. The solvent was removed under reduced pressure to afford a dark red residue which was then placed on a silica gel chromotography column. Compound **5c** was eluted from the column using 10% EtOAc in CH_2Cl_2 as eluant. Compound **5b** is an orange solid (0.576 g., 50%). Orange crystals of **5b** was obtained by slow diffusion of hexane into CH_2Cl_2 and CH_3OH solution of compound **5b**.

Characterization data for 5b

^{1}H-NMR spectrum (500 MHz, acetane-d^6): δ (in ppm)

δ 8.10 (s, 2H, -N*H*-(pc)) and 7.88 (s, 2H, -N*H*-(c)), 7.58 and 6.45 (d, *J* = 2.5 Hz, 4H, -Ar*H*-NH-(pc)), 7.43 and 7.04 (d, *J* = 7.5 Hz, 4H, *m*-Ar*H*, (pc)), 7.12 (d, *J* = 7.5 Hz, 4H, *m*-Ar*H* (c)), 6.95 (t, *J* = 7.5 Hz, 2H, *p*-Ar*H* (c)), 6.89 and 6.82 (t, *J* = 7.5 Hz, 2H, *p*-Ar*H* (pc)), 6.46 (s, 4H, -NH-Ar*H*- (c)) 5.03 and 4.86 (m, 4H, *o*-Cp*H* (pc)), 4.78 (t, *J* = 2 Hz, 4H, *o*-Cp*H* (c)), 4.39-4.37 (m, 4H (m-Cp*H* (pc)), 4H (m-Cp*H* (c)), 8H (-OCH_2-CO-(c and pc)), 4H (AB system(c))), 4.26-4.21 (m, 4H, -OCH_2CH$_3$). 4.07 and 3.05 (d, *J* = 14 Hz, 4H, AB system (pc)), 3.83 and 3.59 (d, *J* = 12.5 Hz, 4H, AB system (pc)), 2.97 (s, 3H, -OCH_3), 1.28 (m, 6H, -CH_3).

ESI-TOF mass spectrum: $C_{50}H_{48}N_2O_{10}Fe$ = 893.51 ([M+H$^+$]) m/z.

Elemental Analysis:

Anal. Calcd. for $C_{50}H_{48}N_2O_{10}Fe \cdot 0.5\ CH_2Cl_2$: C, 64.85; H, 5.28; N, 3.00.
Found: C, 65.28; H, 5.51; N, 3.19.

Melting point: 150 °C

3.2.1.2.13 Preparation of 5,7-diamideferrocenyl-25,26,27,28-tetramethyl ethylestercalix[4]arene (5c)

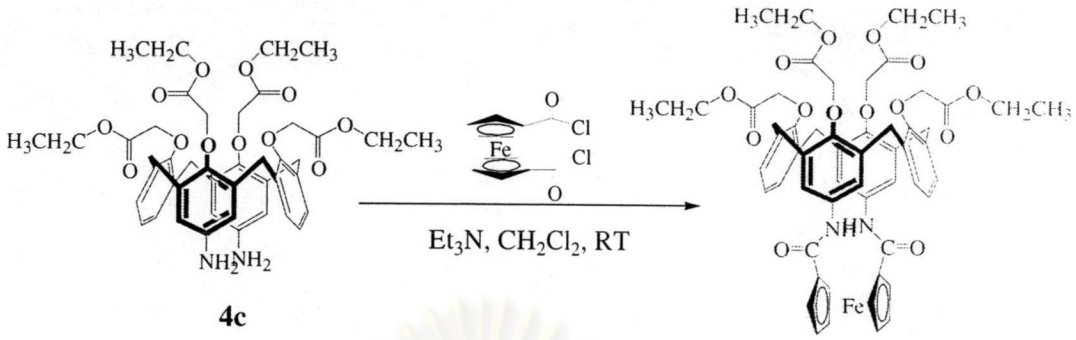

4c **5c**

Into a two-necked round-bottomed flask, the mixture of tetramethylethylester-diaminocalix[4]arene(**4c**) (1.13 g, 1.53 mmol) and triethylamine (1.0 mL) in dichloromethane (40 mL) were stirred at room temperature under N_2. 1,1-Bis (chlorocabonyl)ferrocene (0.481 g, 1.55 mmol) in dichloromethane (20 mL) was transferred into the mixture via cannula. The mixture was stirred at room temperature under N_2 for 4 h. The work-up procedure is similar to the procedure described previously. Crude product was purified on a silica gel column using 10% EtOAc in CH_2Cl_2 as eluant to afford an orange solid **5c** (0.666 g, 42%).

Characterization data for 5c

^{1}H-NMR spectrum (200 MHz, $CDCl_3$): δ (in ppm)

δ 7.25 (s, 2H, -NH-), 7.20 (d, *J* = 6.7 Hz, 4H, m-Ar*H*-OR), 7.09 (t, *J* = 6.4 Hz, 2H, *p*-Ar*H*OR), 6.43 (s, 4H, *o*-Ar*H*-NH-), 4.87 and 3.22 (d, *J* = 13.0, 8H, AB system), 4.90 (s, 4H, -NH-ArHOCH_2-), 4.77 (s, br, 4H,Cp*H*), 4.45 (s, 4H, ArH-OCH_2-), 4.33 (s, br, 4H, Cp*H*), 4.17 (q, *J* = 7.1 Hz, 8H, -OCH_2CH$_3$), 1.33-1.22 (m, 12H, -OCH$_2$CH_3).

ES-TOF mass spectrum: $C_{56}H_{56}N_2O_{14}Fe$ = 1037.20 ([M+H$^+$]) m/z.

Elemental Analysis:

Anal. Calcd. for $C_{56}H_{56}N_2O_{14}Fe$: C, 64.87; H, 5.44; N, 2.70.
Found: C, 64.84; H, 5.40; N, 2.63.

Melting point: 227 °C

3.2.1.2.14 Preparation the variable high temperature experiment of 5a and 5c

Typically, a solution of a ligand (10^{-3}) in DMSO was prepared in an NMR tube. Proton resonances were recorded at variable temperatures, 25 °C, 40 °C, 60 °C, 90 °C, 110 °C, 120 °C, 130 °C, 140 °C and 150 °C for **5a** and 25 °C, 40 °C, 50 °C, 60 °C, 80 °C, 100 °C, 120 °C, 140 °C and 150 °C for **5c**.

3.2.2 Binding studies by NMR titration

3.2.2.1 General Procedure

3.2.2.1.1 Apparatus

^{1}H-NMR spectra were carried out on a Bruker ACF 400 MHz and a Varian 300 MHz nuclear magnetic resonance spectrometer. All anion complexation studies were recorded in acetonitrile-d^6 and chemical shifts referred to a residual proton signal.

3.2.2.1.2 Chemicals

All materials and solvents were standard analytical grade purchased from Aldrich, Fluka, Merck and BDH, and used without further purification unless otherwise noted. Deuterated acetonitrile were stored over 3 Å molecular sieves. All calix[4]arene derivatives were prepared as previously described.

3.2.2.2 Experimental procedure

3.2.2.2.1 ^{1}H-NMR titration studies

3.2.2.2.1.1 Anion binding studies of Ligands (5a), (5b) and (5c) with NBu_4Cl, NBu_4Br, NBu_4I, NBu_4COOCH_3, $NBu_4COOC_6H_5$, $NBu_4H_2PO_4$, NBu_4HSO_4, NBu_4NO_3

Typically, a 0.0033 mol dm^{-3} solution of a ligand ($2x10^{-6}$ mol) in CD_3CN (0.6 mL) was prepared in NMR tubes. A 0.1 mol dm^{-3} stock solution of guest molecules ($5x10^{-5}$ mol) in CD_3CN was prepared in a small vial. The solution of a guest molecule was added into the ligand solution in NMR tube according to the ratios in **Table 3.2.2.2.1**.

Table 3.2.2.2.1 Volumn and concentration of the tetrabutylammonium salts and the ligand used to prepare various tetrabutylammonium salts : ligand ratios.

Mole ratio Guest : Ligand	Volumn of 0.1 M guest in CD_3CN	Concentration of guest molecule	Concentration of Ligand
0.0 : 1.0	0	0	3.333×10^{-3}
0.2 : 1.0	0.004	6.62×10^{-4}	3.331×10^{-3}.
0.4 : 1.0	0.008	1.32×10^{-3}	3.289×10^{-3}
0.6 : 1.0	0.012	1.96×10^{-3}	3.268×10^{-3}
0.8 : 1.0	0.016	2.60×10^{-3}	3.247×10^{-3}
1.0 : 1.0	0.020	3.23×10^{-3}	3.226×10^{-3}
1.2 :1.0	0.024	3.85×10^{-3}	3.205×10^{-3}
1.4 : 1.0	0.028	4.46×10^{-3}	3.185×10^{-3}
1.6 : 1.0	0.032	5.06×10^{-3}	3.165×10^{-3}
1.8 : 1.0	0.036	5.66×10^{-3}	3.145×10^{-3}
2.0 : 1.0	0.040	6.25×10^{-3}	3.125×10^{-3}
2.5 : 1.0	0.050	7.69×10^{-3}	3.077×10^{-3}
3.0 : 1.0	0.060	9.10×10^{-3}	3.030×10^{-3}
3.5 : 1.0	0.070	1.04×10^{-2}	2.985×10^{-3}
4.0 : 1.0	0.080	1.18×10^{-2}	2.941×10^{-3}

3.2.2.2.1.2 Cation binding studies of Ligands (5b) and (5c) with $NaClO_4$, KPF_6, $CsPF_6$, $RbPF_6$.

Typically, a 0.0033 mol dm^{-3} solution of a ligand ($2x10^{-6}$ mol) in CD_3CN (0.6 mL) was prepared in NMR tubes. A 0.1 mol dm^{-3} stock solution of cation molecules ($5x10^{-5}$ mol) in CD_3CN was prepared in a small vial. The solution of a cation molecule was added into the ligand solution in NMR tube according to ratios in **Table 3.2.2.2.2**.

Table 3.2.2.2.2 Volumn and concentration of a cation salt and the ligand used to prepare various cation salt : ligand ratios.

Mole ratio Guest : Ligand	Volumn of 0.1 M guest in CD_3CN	Concentration of guest molecule	Concentration of Ligand
0.0 : 1.0	0	0	$3.333x10^{-3}$
0.2 : 1.0	0.004	$6.62x10^{-4}$	$3.331x10^{-3}$.
0.4 : 1.0	0.008	$1.32x10^{-3}$	$3.289x10^{-3}$
0.6 : 1.0	0.012	$1.96x10^{-3}$	$3.268x10^{-3}$
0.8 : 1.0	0.016	$2.60x10^{-3}$	$3.247x10^{-3}$
1.0 : 1.0	0.020	$3.23x10^{-3}$	$3.226x10^{-3}$
1.2 :1.0	0.024	$3.85x10^{-3}$	$3.205x10^{-3}$
1.4 : 1.0	0.028	$4.46x10^{-3}$	$3.185x10^{-3}$
1.6 : 1.0	0.032	$5.06x10^{-3}$	$3.165x10^{-3}$
1.8 : 1.0	0.036	$5.66x10^{-3}$	$3.145x10^{-3}$
2.0 : 1.0	0.040	$6.25x10^{-3}$	$3.125x10^{-3}$
2.5 : 1.0	0.050	$7.69x10^{-3}$	$3.077x10^{-3}$
3.0 : 1.0	0.060	$9.10x10^{-3}$	$3.030x10^{-3}$
3.5 : 1.0	0.070	$1.04x10^{-2}$	$2.985x10^{-3}$

3.2.2.2.1.3 Simutanious cation and anion binding studies of Ligands (5b).

Typically, the mixture of a 0.0033 mol dm^{-3} solution of a ligand ($2x10^{-6}$ mol) and cation species ($2x10^{-6}$ mol) in CD_3CN (0.6 mL) was prepared in NMR tubes. A 0.1 mol dm^{-3} solution of a anion molecule ($5x10^{-5}$ mol) in CD_3CN was prepared. The stock solution of anion molecule was added into the mixture solution in NMR tube according to 0-4.0 equivalence in **Table 3.2.2.3**.

Table 3.2.2.2.1.3 Volumnes and concentration of the tetrabutylammonium salts and the solution of ligand and cation used to prepare various tetrabutylammonium salts : the ligand ratios.

Mole ratio Guest : Ligand	Volumn of 0.1 M guest in CD_3CN	Concentration of guest molecule	Concentration of Ligand
0.0 : 1.0	0	0	$3.333x10^{-3}$
0.2 : 1.0	0.004	$6.62x10^{-4}$	$3.331x10^{-3}$.
0.4 : 1.0	0.008	$1.32x10^{-3}$	$3.289x10^{-3}$
0.6 : 1.0	0.012	$1.96x10^{-3}$	$3.268x10^{-3}$
0.8 : 1.0	0.016	$2.60x10^{-3}$	$3.247x10^{-3}$
1.0 : 1.0	0.020	$3.23x10^{-3}$	$3.226x10^{-3}$
1.2 :1.0	0.024	$3.85x10^{-3}$	$3.205x10^{-3}$
1.4 : 1.0	0.028	$4.46x10^{-3}$	$3.185x10^{-3}$
1.6 : 1.0	0.032	$5.06x10^{-3}$	$3.165x10^{-3}$
1.8 : 1.0	0.036	$5.66x10^{-3}$	$3.145x10^{-3}$
2.0 : 1.0	0.040	$6.25x10^{-3}$	$3.125x10^{-3}$
2.5 : 1.0	0.050	$7.69x10^{-3}$	$3.077x10^{-3}$
3.0 : 1.0	0.060	$9.10x10^{-3}$	$3.030x10^{-3}$
3.5 : 1.0	0.070	$1.04x10^{-2}$	$2.985x10^{-3}$
4.0 : 1.0	0.080	$1.18x10^{-2}$	$2.941x10^{-3}$

3.2.3 Electrochemical studies

3.2.3.1 General procedure

3.2.3.1.1 Apparatus

Cyclic Votammetry and Square Wave Voltammetry were performed using an AUTOLAB PGSTAT 100 potentiostat. All electrochemical experiments were carried out in a three-electrode cell designed in-house comprising of a working electrode, a counter electrode and a reference electrode. The working electrode was a glassy carbon disk with a diameter of 6 mm embedded in Teflon and the counter electrode was a platinum coil. $Ag/AgNO_3$ electrodes were used as a reference electrode in acetonitrile solution.

The counter electrode, platinum wire, was polished with a sandpaper prior to use. A $Ag/AgNO_3$ electrode was customarily constructed by immersing a silver wire into a solution of 0.01 mol dm^{-3} $AgNO_3$ in 0.1 mol dm^{-3} supporting electrolyte. The working electrode was polished with slurries of 0.5 μm and 1 μm alumina powder, and washed by sonication for 5 min in 0.05 mol dm^{-3} sulfuric acid and subsequently with a solvent.[84] Solutions were kept under N_2 at all time. Scan rates were carried at 20, 50, 80, 100, 200, 500, 800 and 1000 mV/s. The appropriated scan rates were found to be 50 and 100 mV/s for cyclic voltammetry, and at 50 mV/s for square wave voltammetry.

3.2.3.1.2 Chemicals

All guest molecules in terms of tetrabutylammonium salts and supporting electrolyte, tetrabuthlammonium hexafluorophosphate, were dried under reduced pressure overnight. Acetonitrile was dried over KOH pellets overnight and subsequently distilled with CaH_2 under N_2 prior to used.

3.2.3.2 Experimental procedure

3.2.3.2.1 Anion and cation binding studies of Ligands (5a), (5b) and (5c) with NBu_4COOCH_3, $NBu_4COOC_6H_5$, $NBu_4H_2PO_4$ and NBu_4Cl and those of 5c and $NaClO_4$

Typically, a 0.001 mol dm^{-3} solution of a ligand ($5x10^{-6}$ mol) in 0.1 mol dm^{-3} supporting electrolyte (5 mL of NBu_4PF_6 in freshly distilled CH_3CN) was prepared. A stock solution (0.1 mol dm^{-3}) of an anionic or cationic species ($5x10^{-4}$ mol) in supporting electrolyte was prepared. The solution of an anion or cation was added into the solution of the ligand according to the ratios in the **Table 3.2.3.2.1**.

Table 3.2.3.2.1 Volumnes and moles of $NaClO_4$ used for a typical CV experiment

Mole ratio Guest : Ligand	Volumn of 0.1 M guest in CD_3CN	Mole of guest molecule
0.0 : 1.0	0	0
0.2 : 1.0	0.010	1.0x10-6
0.4 : 1.0	0.020	$2.0x10^{6}$
0.6 : 1.0	0.030	$3.0x10^{-6}$
0.8 : 1.0	0.040	$4.0x10^{-6}$
1.0 : 1.0	0.050	$5.0x10^{-6}$
1.2 :1.0	0.060	$6.0x10^{-6}$
1.5 : 1.0	0.075	$7.5x10^{-6}$
1.8: 1.0	0.090	$9.0x10^{-6}$
2.0 : 1.0	0.100	$1.0x10^{-5}$
2.5 : 1.0	0.125	$1.25x10^{-5}$
3.0 : 1.0	0.150	$1.50x10^{-5}$
4.0 : 1.0	0.200	$2.0x10^{-5}$

3.3. Results and Discussion

3.3.1 Synthesis and Characterization of calix[4]arene derivatives

3.3.1.1 Design and Syntheses

Our research group has interested in the design and synthesis of molecules which can function as sensors. Basic sensory units giving electrochemical signals such as ferrocene[79], cobaltocenium[80], quinone[81], tetrathiafulvalene[82], viologen[83] are well-known. We have designed anion receptors containing ferrocene units connecting to the amide moieties. The amide groups bind with anion guests using hydrogen bonding interactions: O=C-N-H---X, where X = anions. Nevertheless, we have attached ethyl ester groups on the lower rim of calix[4]arene to function as rotation-inhibitors as well as binding sites for cations. The designed molecules are shown in **Figure 3.3.1**.

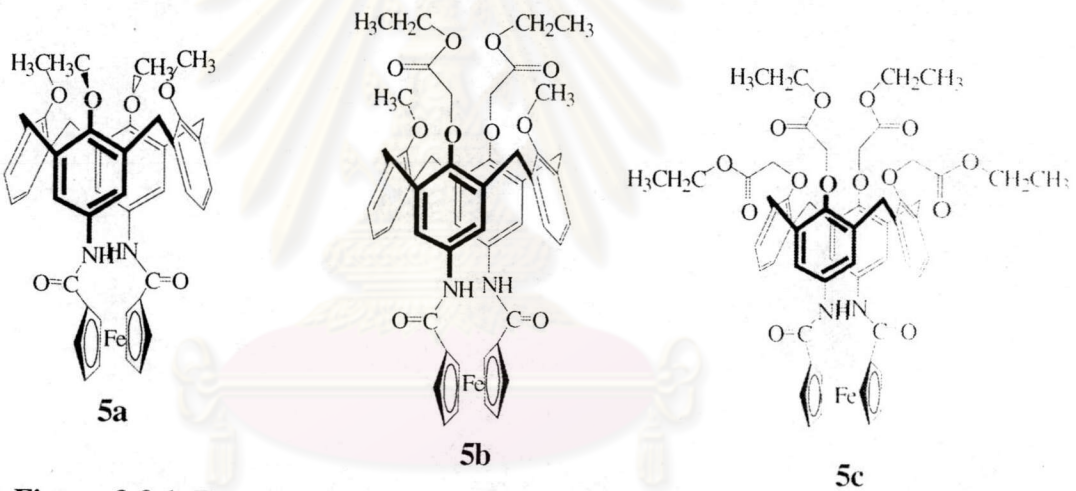

Figure 3.3.1 Target molecules contain cation and anion binding sites

Syntheses of ethyl ester ferrocene amide and methoxy ferrocene amide calix[4] arene **5a**, **5b** and **5c** are summarized in **Scheme 3.3.1**. Nitrations of dimethoxy calix[4] arene**1a**[77] and diethyl ester calix[4]arene **1b**[84] were accomplished using a phase transfer strategy[85] between organic and water phase. $NaNO_3$, concentrated HCl and $La(NO_3)_3$ as catalyst were dissolved in water while compounds **1a** and **1b** were dissolved in dichloromethane. The solution mixture was kept stirring vigorously at room temperature until thesolution turned yellow. The mixture were worked up to afford yellow powders of dimethoxy dinitrocalix[4]arene (**2a**) and diethyl ester dinitrocalix[4]arene (**2b**) in 71% and 88%, respectively. Reagents used in this reaction are mind and appropriate for producing selectively nitro substituents on the *para* position of phenol rings . Compound **2a** hardly dissolves in common solvents such as CH_2Cl_2, CH_3OH, EtOAc and CH_3CN.

but dissolves very well in DMF. Thus, the nucleophilic substitutions of compound **2a** with CH_3I and ethyl bromoacetate in the presence of NaH and K_2CO_3, respectively, were carried out in DMF at 60 °C. Controlling the temperature for this reaction is quite important because DMF can decompose at higher temperature. The tetra-substituted dinitrocalix[4]arene, **3a** and **3b,** were obtained as pale-yellow powders at 71% and 61% yields, respectively. On the other hand, diethyl ester dinitrocalix[4]arene dissolves easily in common organic solvents. Nucleophilic substitution of **2b** with ethyl bromoacetate was carried out in acetonitrile in the presence of Na_2CO_3. Pale-yellow solid of tetraethyl esterdinitrocalix[4]arene (**3c**) was obtained in 61% yield. Essentially, the hydroxy groups at the *para* position to the nitro groups must be protected prior to the reduction of nitro groups to amino groups because *p*-hydroxy aniline unit is easy to be oxidized and transformed to quinone. Reduction of nitro groups (**3a**, **3b** and **3c**) was carried out using Raney Ni and $N_2H_4{\cdot}H_2O$ in the mixture of CH_3OH and EtOAc to yield diamino compounds **4a**, **4b** and **4c** in 98%, 95%, and 96% yields, respectively.[86] Coupling reactions were performed using the freshly synthesized diamino compounds (**4a**, **4b** and **4c**) and 1,1-bis(chlorocarbonyl)ferrocene[87-88] This reaction should be refrained from the moisture because the hydroxy group can replace the Cl atom of chlorocarbonylferrocene to give carboxylic ferrocene. Therefore, 1,1-bis(chlorocarbonyl)ferrocene were maintained under N_2 and transferred via cannula to the solution of diamino calix[4]arene in the presence of NEt_3 in CH_2Cl_2. The mixture was stirred at room temperature under N_2 for 4 h to produce orange solids of ferrocene amide calix[4]arenes **5a**, **5b** and **5c** in 50%, 42%, and 40% yields, respectively. The main by-product from this reaction is Bisamideferrocene calix[4]arene. In order to achieve higher yields of the desired compounds, reactions should be carried out in dilute solutions.

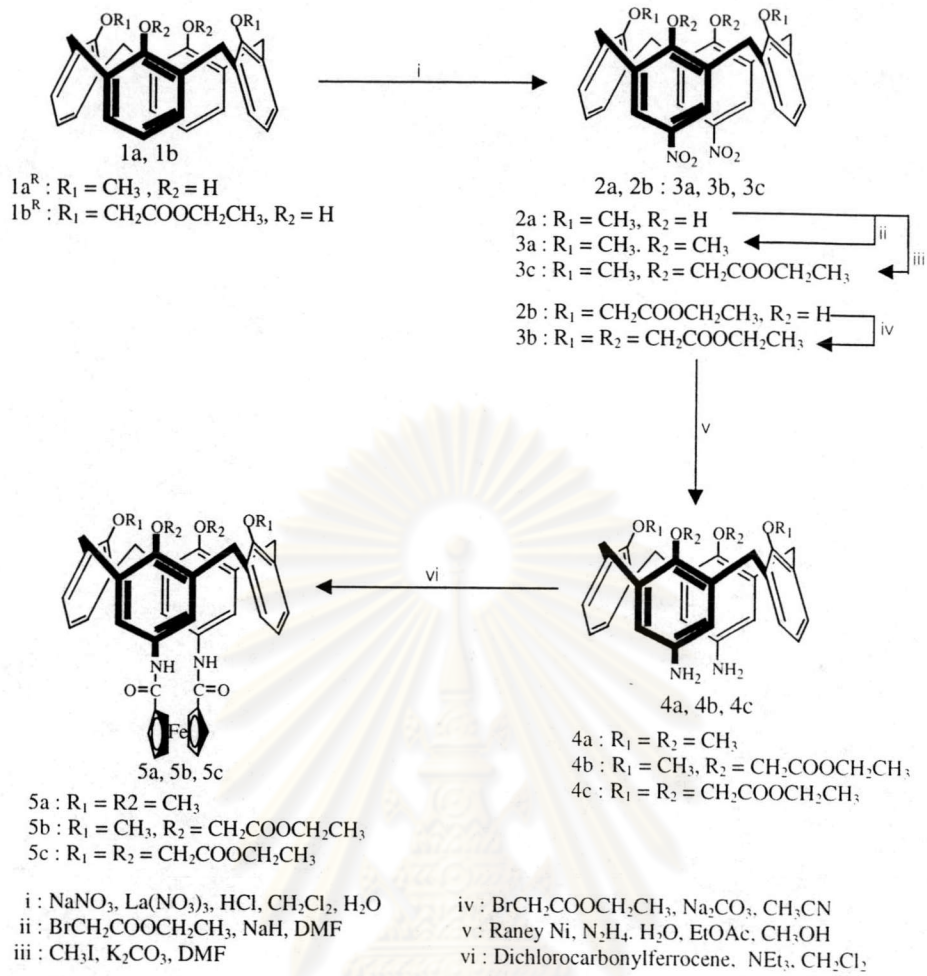

Scheme 3.3.1 Pathway of syntheses **5a**, **5b** and **5c**

3.3.1.2 Structure in Solution and Solid State

The structures of calix[4]areneare are normally classified into four basic conformations according to the possible 'up' and 'down' arrangement of the phenol rings: cone, partial cone, 1,2-alternate and 1,3-alternate. The most stable conformation is cone conformation due to intramolecular hydrogen bonding among hydroxy groups at the lower rim. However, calix[4]arene compounds are found in other conformations depending on the base used in substitution reactions and functional groups attached on the lower rim oxygen atoms.[89] In the case of compounds **5a** and **5b**, NMR spectra at room temperature showed complicated signals suggesting a mixed conformation of the calix[4] arene unit. Both compounds have two opposite anisole rings in a rigid fashion linking by amide ferrocene and the remianed phenyl rings are flexible for free rotation. ^{1}H-NMR spectra of both **5a** and **5b** exhibited sharp peaks at room temperature (**Figure 3.3.5, and 3.3.6**) suggesting that the conformational interconversion took place in a slow exchange

manner on NMR time scale.[90] According to COSY, NOESY, ROESY, HMQC, HMBC and DEPT, both cone and partial cone conformation were seen in the spectrum. For the most advantage of the mentioned 2D-NMR techniques above, the correlation cross peaks of NOESY can be used to identify corresponding 2 different conformations in the spectrum. The correlation of signals can be assigned either cone or partial cone conformation. The correlation protons were assigned in **Figure 3.3.2** according to the results of NOESY shown in **Figure 3.3.3 and 3.3.4.**

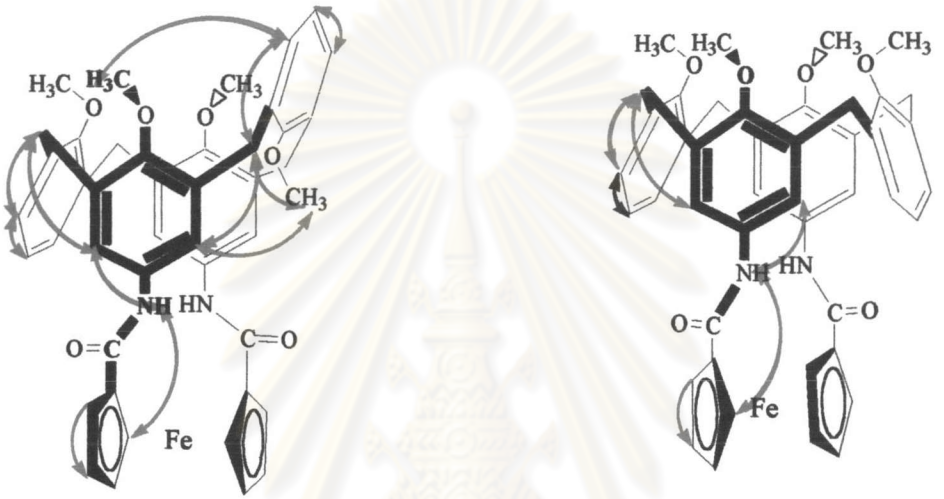

Partial Cone conformation Cone conformation

Figure 3.3.2 NOESY correlation of Partial Cone and Cone conformation of **5a**

From the 2D-NOESY correlation of the partial cone conformation, the methoxy group at 2.87 ppm on the rotated phenol ring displays a cross peak with *o*-Ar*H*NHCO aromatic proton at 6.379 ppm. The other methoxy groups correlates to the inversed aromatic protons (doublet signals at 7.20 and 7.06 ppm and triplet signals at 6.90 and 6.63 ppm).

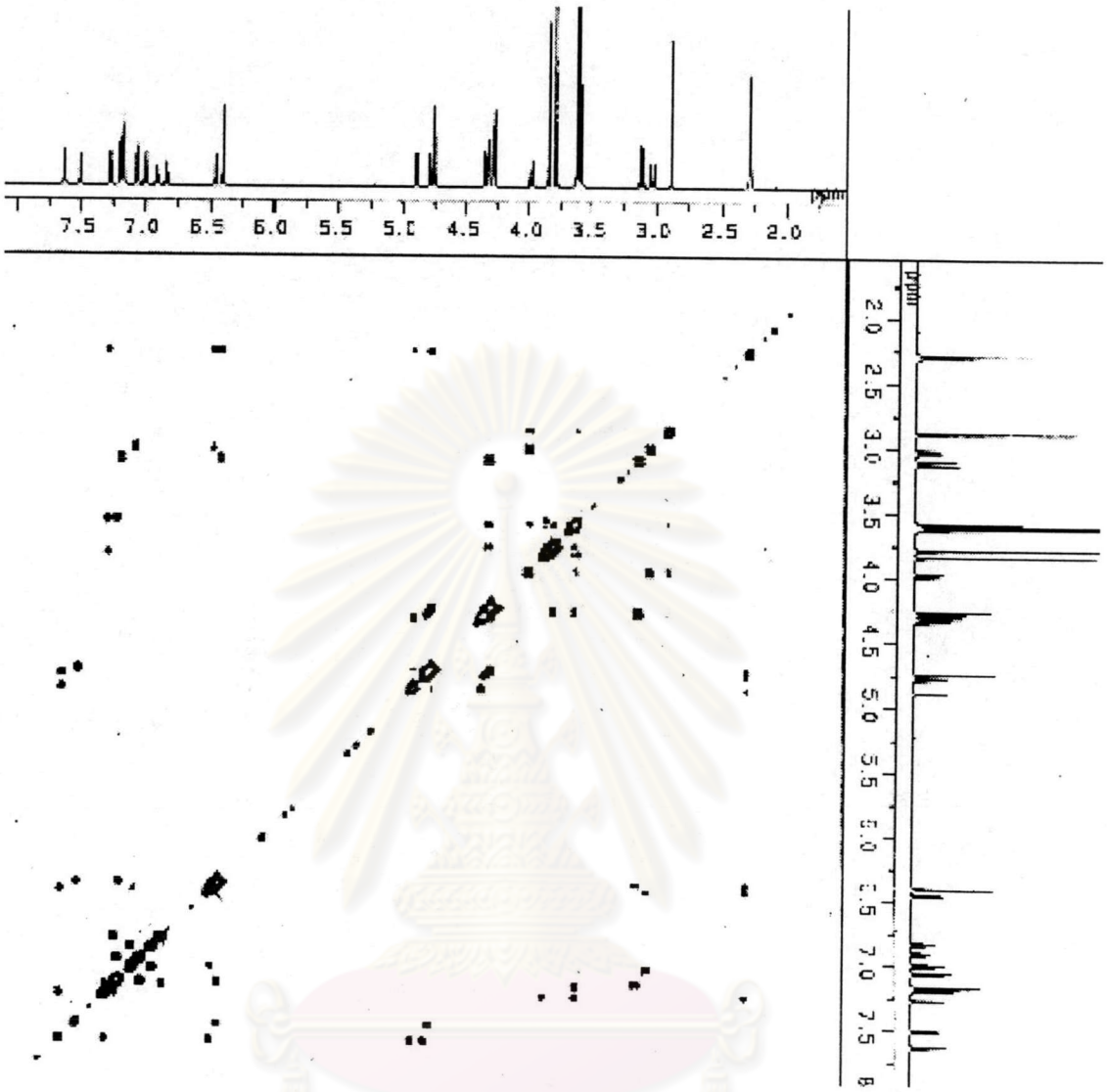

Figure 3.3.3 NOESY spectrum of 5,7-diamideferrocenyl-25,26,27,28-tetramethoxycalix [4]arene (**5a**) in $CDCl_3$ with 400 MHz

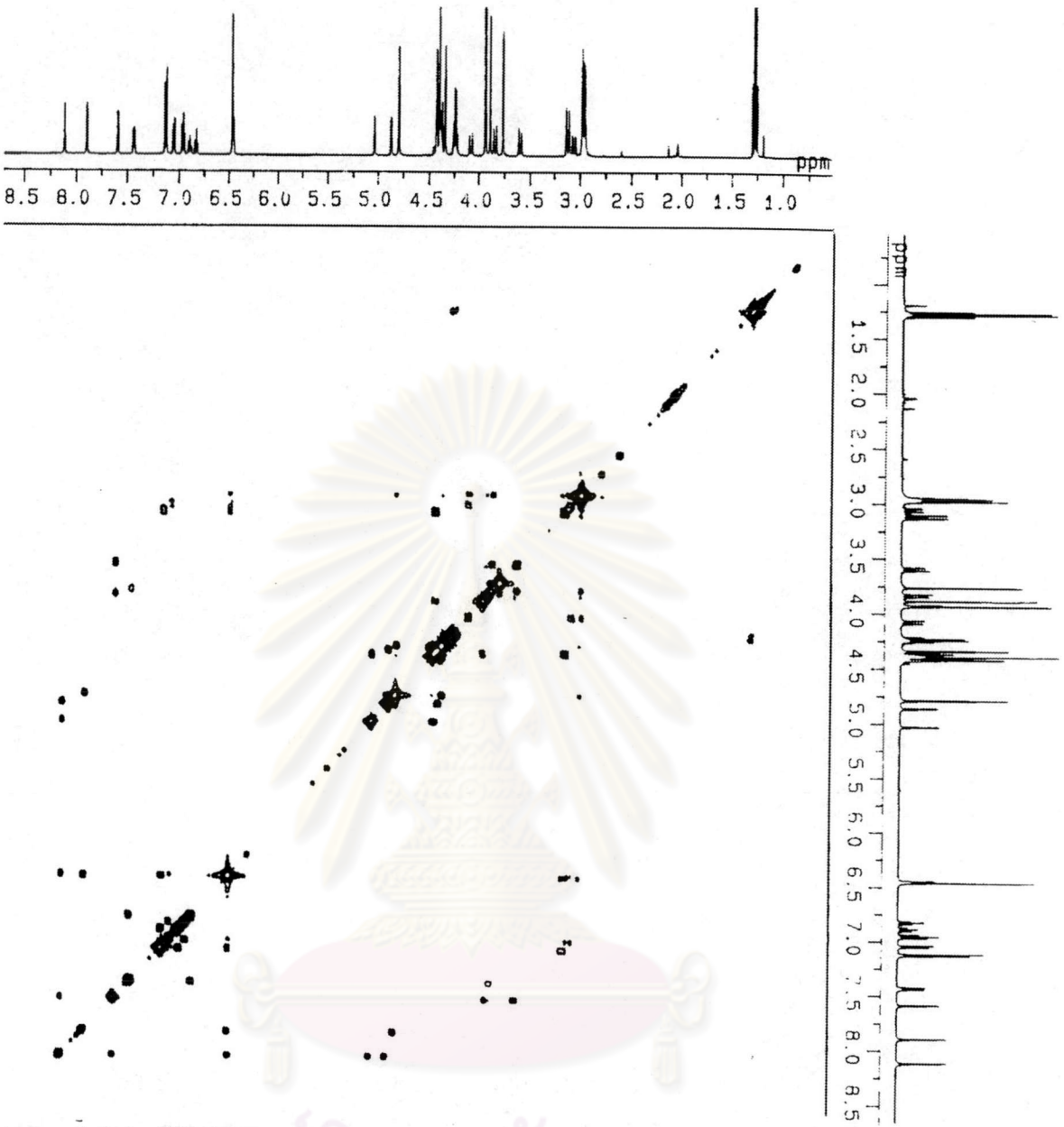

Figure 3.3.4 NOESY spectrum of 5,7-diamideferrocenyl-25,26,27,28-dimethoxy dimethyl ethylestercalix[4]arene (**5b**) in Acetone-d^6 with 500 MHz

The methylene protons at 3.98 ppm correlate to the methoxy group on the inversed aryl ring. On the other hand for cone conformation, the methoxy groups have no correlation with the aromatic protons and with the methylene protons. In contrast to **5a** and **5b**, tetraethylester calix[4]arene (**5c**) was found to be in a cone conformation only in the solution state. Four bulky ethylester groups at the lower rim thus inhibit the ring rotation.

Considering the ^{1}H-NMR spectra of **5a** and **5b** in acetone-d^6, 500 MHz, the cone conformation has two planes of symmetry. The aromatic protons exhibit a triplet for *p*-Ar*H*OCH$_3$ at 7.01 ppm for **5a** and at 6.95 ppm for **5b**, a doublet of *m*-Ar*H*OCH$_3$ at 7.22

ppm for **5a** and at 7.12 ppm for **5b** and a singlet for meta protons substituted aromatic ring on upper rim at 6.47 ppm for **5a** and at 6.46 ppm for **5b**. In addition, the methylene bridge protons in cone conformation appear as two sets of doublets at 4.36 and 3.14 ppm for **5a** and at 4.04 and 3.06 ppm for **5b** while partial cone conformation has 4 sets of doublets at 4.29, 3.98, 3.11 and 3.03 ppm for **5a** and at 4.09, 3.82, 3.32 and 3.19 ppm for **5b**. It is notable that peaks due to methyl protons of the partial cone conformation shift more up-field shift than those of the cone conformation. This probably stems from the effect of ring currents from aryl units of calix[4]arene when one of the methoxy group point into the calix[4]arene cavity (**Figure 3.3.5 and 3.3.6**) Additionally, ^{13}C NMR spectra of compounds **5a** and **5b** show characteristic peaks of methylene bridge carbon at ca. 31 ppm for the cone conformation and at ca. 31 ppm and ca. 37 ppm for partial cone conformation.[91]

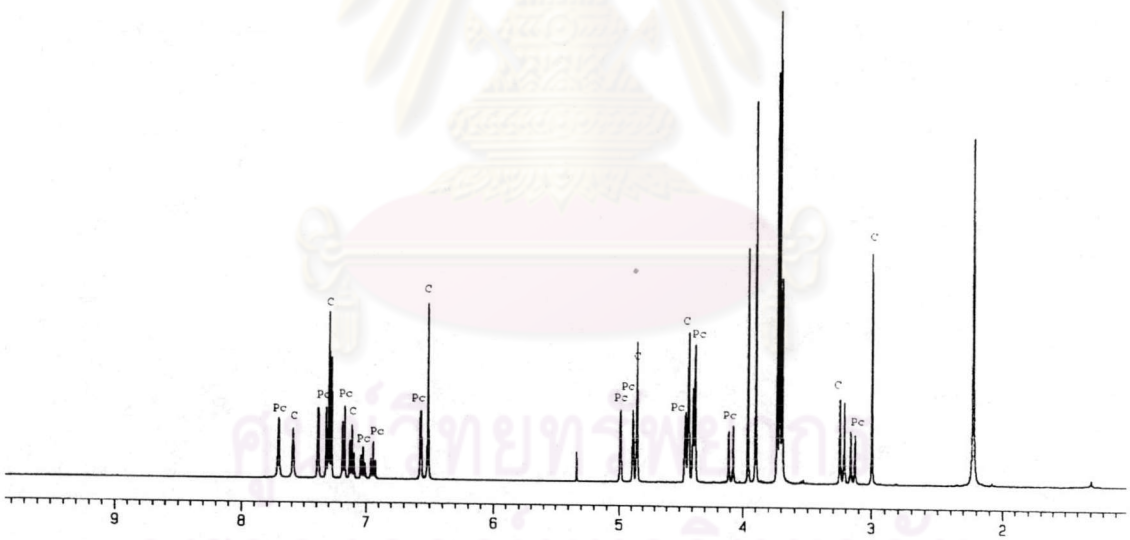

Figure 3.3.5 ^{1}H-NMR spectrum of 5,7-diamideferrocenyl-25,26,27,28-tetramethoxycalix [4]arene (**5a**) in $CDCl_3$ with 400 MHz

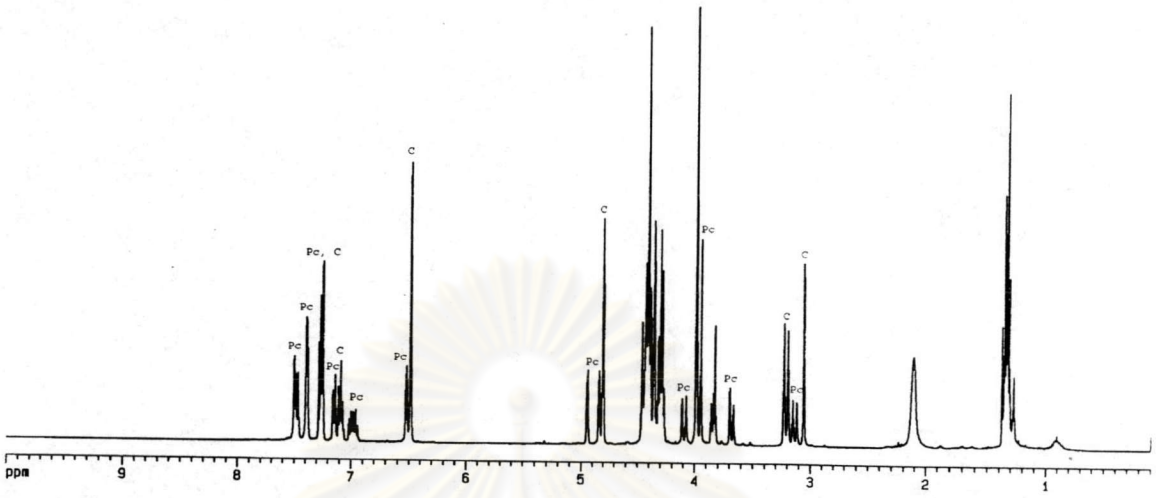

Figure 3.3.6 ^{1}H-NMR spectrum of 5,7-diamideferrocenyl-25,26,27,28-dimethoxy dimethyl ethylestercalix[4]arene (**5b**) in $CDCl_3$ with 400 MHz

^{1}H-NMR spectra of **5a** and **5b** in the different solvents show the different intensity of cone and partial cone conformation ratio depending on the polarity of solvent. (Shown in **Table 3.3.1**)

Table 3.3.1 Show the intensity of cone and partial cone conformation ratio

	5a C:PC	**5b** C:PC
$CDCl_3$	1:1	1:1
CD_2Cl_2	1:1	1:1
Acetone-d^6	1:2	1:1
DMSO-d^6	1:2	1:1
CD_3CN-d^3	1:1	1:1

Elucidation of ^{1}H-NMR spectra of **5a** and **5b** in DMSO-d^6 and acetone-d^6 was found that compound **5a** exists in partial cone and cone conformation in 2:1 ratio, whereas compound **5b** in 1:1 ratio. The ratio of cone to partial cone conformation for **5a** and **5b** is 1:1 in CD_3Cl and CD_2Cl_2. This is opposite to that reported by Shikai where the concentration of cone conformation of tetramethoxy calix[4]arene was found to increase

upon increasing solvent polarity.[92] From the ^{1}H-NMR spectrum of **5c**, it shows only cone conformation containing a triplet for *p*-Ar*H*OCH$_3$ at 7.09 ppm, a doublet of *m*-Ar*H*OR at 7.20 ppm and a singlet for meta protons substituted aromatic ring on upper rim at 6.43 ppm as well as the methylene bridge proton at 4.87 and 3.22 ppm as shown in **Figure 3.3.7**.

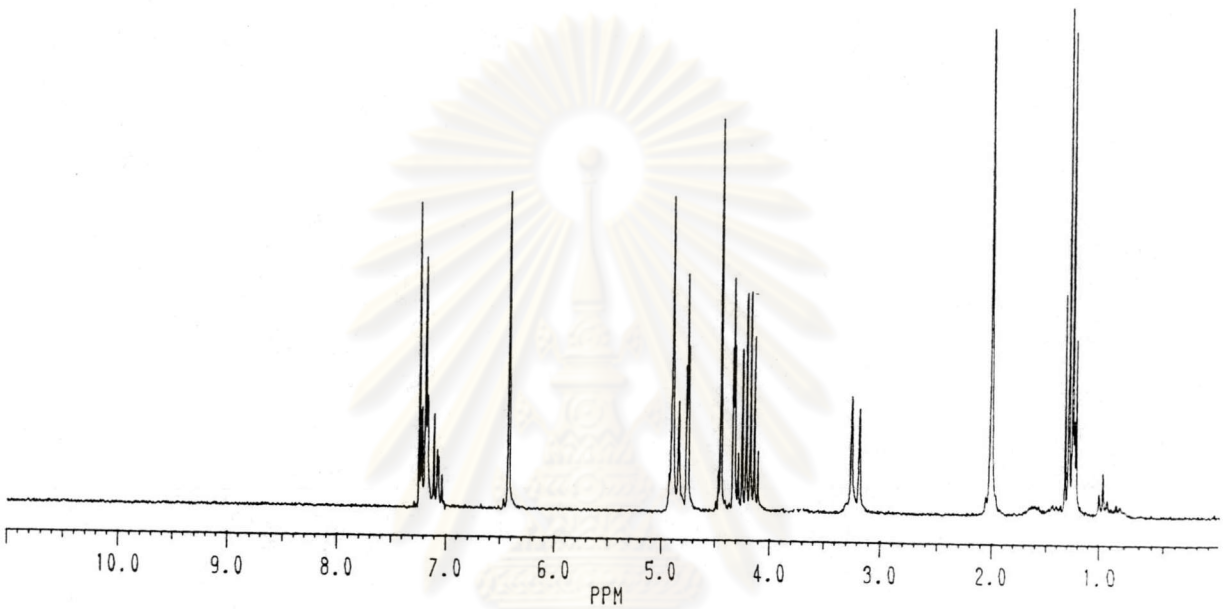

Figure 3.3.7 ^{1}H-NMR spectrum of 5,7-diamideferrocenyl-25,26,27,28-tetramethyl ethylestercalix[4]arene (**5c**) in $CDCl_3$ with 200 MHz

3.3.1.3 VT NMR experiments

Conformational interconversion can be studied by variable temperature NMR spectroscopy in order to investigate the inversion barrier energy between cone and partial cone conformation.[93-96] ^{1}H-NMR spectra of **5a** and **5c** exhibit sharp signals at room temperature indicating a slow exchange of conformation on the NMR time scale.[97] In order to study thermodynamic properties of these receptors (**5a** and **5b**), they should, thus, be determined by measuring dynamic ^{1}H-NMR at high temperature in DMSO-d^6 ranging from 25 to 150 °C (which is the limitation of the NMR machine and solvent properties). Variable temperature ^{1}H-NMR spectra is illustrated in **Figure 3.3.8**. No coalescence signals were observed in the range of 25-150 °C.

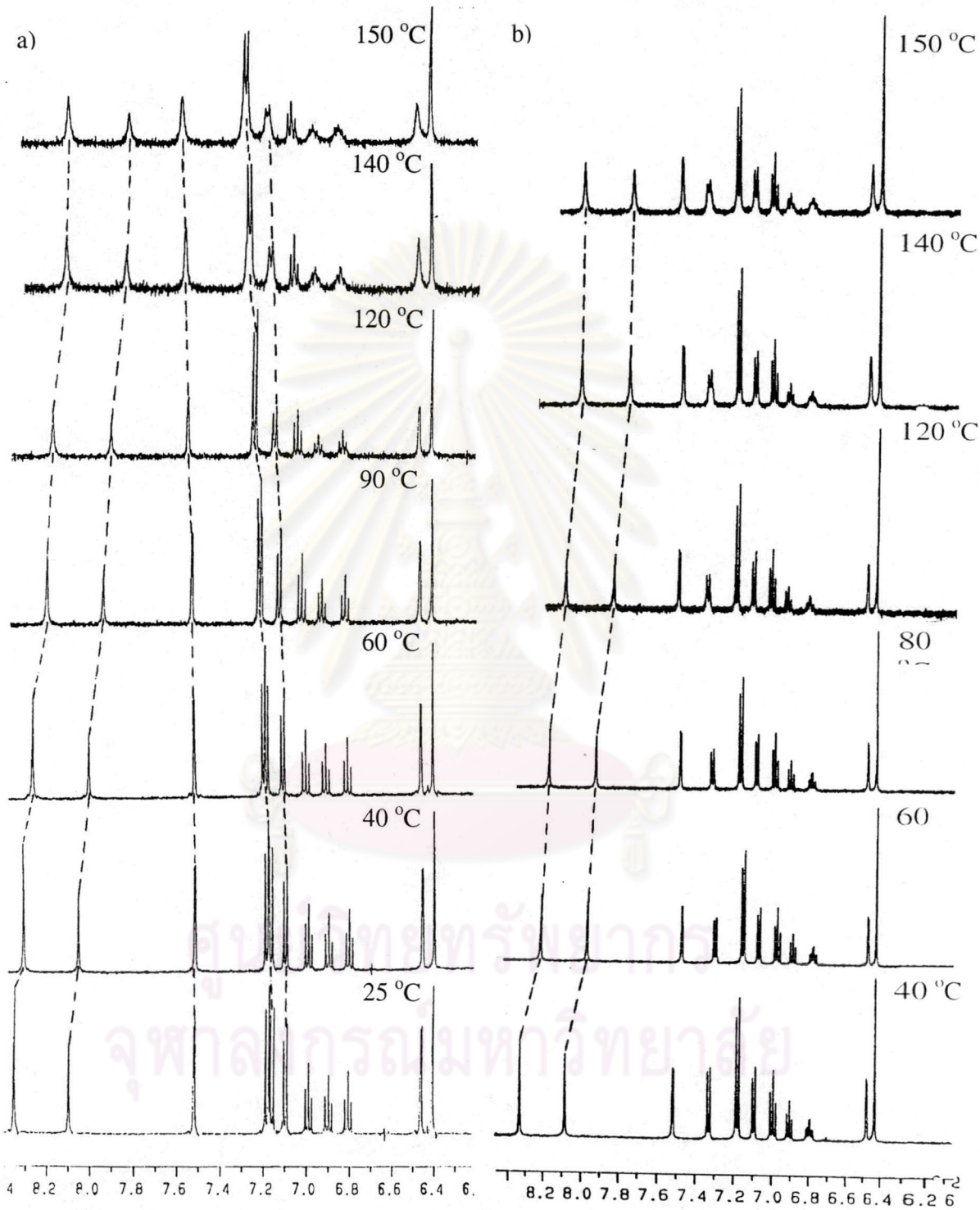

Figure 3.3.8 Variable high temperatures of **5a** (a) and **5b** (b) in DMSO-d^6

The NH peaks of **5a** and **5b** in cone and partial cone conformation move up field (**5a**; $\Delta\delta$ = 0.438 and 0.441 ppm for C and Pc, respectively, **5b**; $\Delta\delta$ = 0.43 for both C and PC) and doublet peaks at ArCH_2Ar of partial cone conformation shifted downfield

slightly ($\Delta\delta \sim 0.1$ ppm). All peak assignments of partial cone conformation for **5a** became board at 110 °C and their intensities decreased while those of **5b** took place at 140 °C. This signified that the methoxy aromatic rings of **5b** rotated around methylene bridge more slowly than those of **5a** since compound **5b** had two bulky ethyl ester groups to inhibit the rotation. In contrast, cone conformation for both **5a** and **5b** retained sharp signals even at higher temperature. It implies that cone conformation is stable and does not undergo interconversion at high temperature.[98] According to integrated signals, partial cone conformation gradually changed to cone conformation observed from reduction of mole fractions of PC whereas those of C increased at higher temperature. **(Figure 3.3.9)**

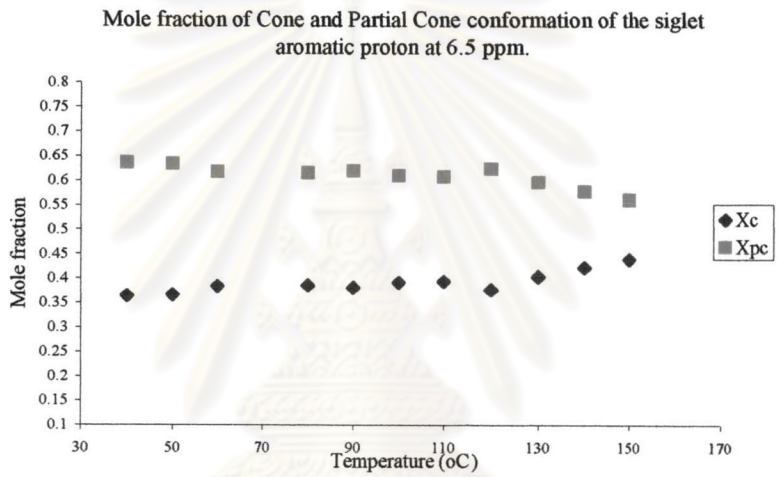

(a) Mole fraction of Tetramethoxyamideferrocenecalix[4]arene **5a**

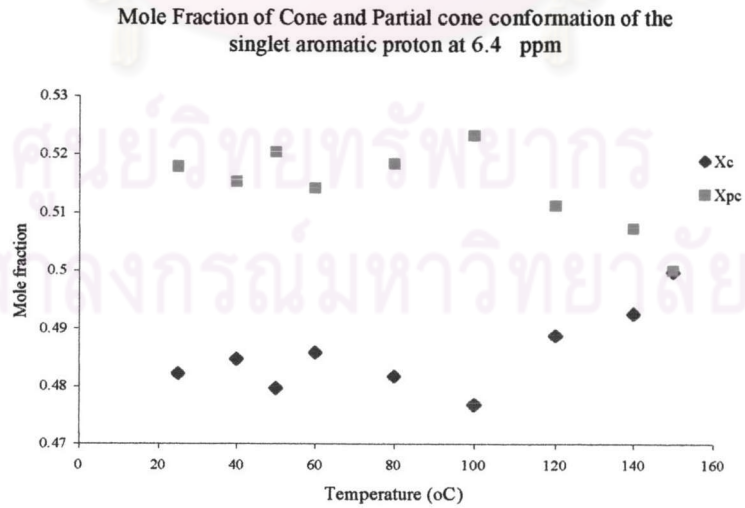

(b) Mole fraction of Dimethoxydimethylethylesteramideferrocenecalix[4]arene **5c**

Figure 3.3.9 Mole fraction of cone and partial cone conformation at variable temperature from 25 °C to 150 °C

Reinhoudt et al.[98] studied the mechanism of conformational interconversion of calix[4] arene derivatives containing tetramethoxy at lower rim and crown-ether at upper rim by quantitative 2-D EXSY NMR spectroscopy. (**Figure 3.3.10**)

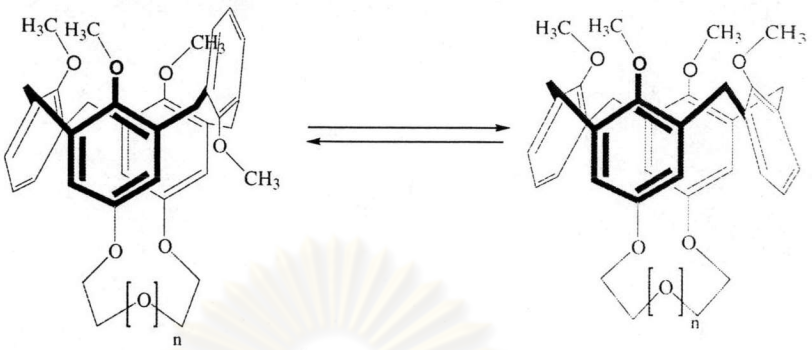

Partial Cone Conformation　　Cone Conformation

Figure 3.3.10 Tetramethoxy calix[4]crown in cone and partial cone conformation

Behaviors of ^{1}H-NMR spectra of their compounds are similar to ^{1}H-NMR spectra of both **5a** and **5b** shich showrd sharp signals of the mixture of cone and partial cone conformation at room temperature. Surprisingly, the results of 2-D EXSY NMR spectrum showed that the conformational interconversion processes occur via the intermediate of 1,3-alternate conformation following the equilibrium shown in **3.3.1**.

$$C \underset{k_{PC}}{\overset{k_{CP}}{\rightleftharpoons}} A \underset{k_{AP}}{\overset{k_{PA}}{\rightleftharpoons}} P \qquad (3.3.1)$$

Reinhoudt stated that this mechanism cannot be observed by ^{1}H-NMR and 2D-NOSEY results.

It is worthwhile to propose that the mechanism of **5a** and **5b** may occur pass the 1,3-alternate conformation. Otherwise the conformational interconversion took place possibly between cone and partial cone conformation directly. Variable high temperature results give enough information to deduce that the conformational interconversion of **5a** and **5b** took place between cone to partial cone without the intermediate 1,3-alternate conformation. (**Figure 3.3.11**)

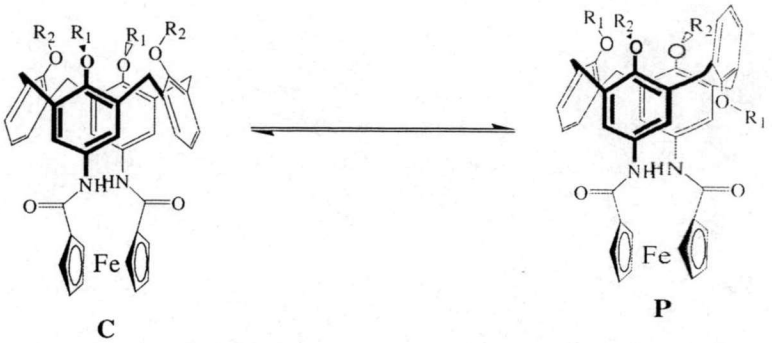

5a ; R_1=R_2= CH_3
5b ; R_1=CH_3, R_2= $CH_2COOCH_2CH_3$

Figure 3.3.11 The proposed mechanism of conformational interconversion of **5a** and **5c**

3.3.1.4 X-ray structure analysis

Crystals of **5a** and **5b** were obtained by slow diffusion of hexane to the solution of compounds **5a** and **5b** in mixed CH_2Cl_2 and CH_3OH. Crystallographic data are listed in **Table 3.3.2**.

Table 3.3.2 Crystallographic data for the X-ray Diffraction Studies of **5a** and **5b**

Compounds	**5a**	**5b**
Empirical Formula	$C_{46}H_{48}FeN_2O_8$	$C_{52}H_{56}FeN_2O_{12}$
Formula weight	812.71	956.84
Temperature (K)	120 (2)	120(2)
Radiation (λ, Å)	Mo Kα (0.71073)	Mo Kα (0.71073)
Crystal system	Monoclinic	Monoclinic
Space group	$P2_1$	$C2/c$
a, (Å)	12.813(3)	13.008(3)
b, (Å)	13.337(3)	21.775(4)
c, (Å)	12.983(3)	16.105(3)
α = γ, deg	90	90
β, deg	118.73(3)	95.48(3)
V, $Å^3$	1945.5(7)	4540.9
Z	2	4
ρ(cal), g/cm^3	1.387	1.400

Abs coeff, (mm^{-1})	0.447	0.401
Crystal size (mm^3)	0.20 x 0.18 x 0.14	0.26 x 0.14 x 0.12
Reflection collected	15395	20610
$R(F)^a$, %	5.69	4.59
$Rw(F^2)^a$, %	14.17	11.39

[a]Residuals: $R(F) = \Sigma| F_o-F_d | /\Sigma F_o$; $R_w(F^2) = \{[\Sigma w(F_o^2-F_c^2)^2]/[\Sigma w(F_o^4)^2]\}^{1/2}$.

Compound **5a** has 2 molecules of CH_3OH as a solvent of crystallization while **5b** contains 1 molecule of CH_3OH. There are hydrogen bonding interactions between C=O of the amide group and hydrogen atom of methanol and also between NH of the amide group and oxygen atom of methanol as shown in **Figure 3.3.12**.

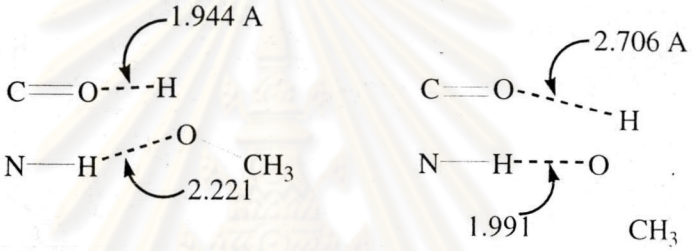

Hydrogen bond interactions between methanols and amide group of **5a**

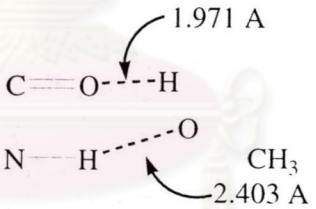

Hydrogen bond interactions between methanol and amide group of **5b**

Figure 3.3.12 The distance of hydrogen bond interaction between methanol and amide group of **5a** and **5c**

X-ray structures showed that the compound **5a** adopts a partial cone conformation in the solid state, in which all methoxy groups point out of cavity. This reduces the steric crowdedness of the calix[4]arene units.[99-100]

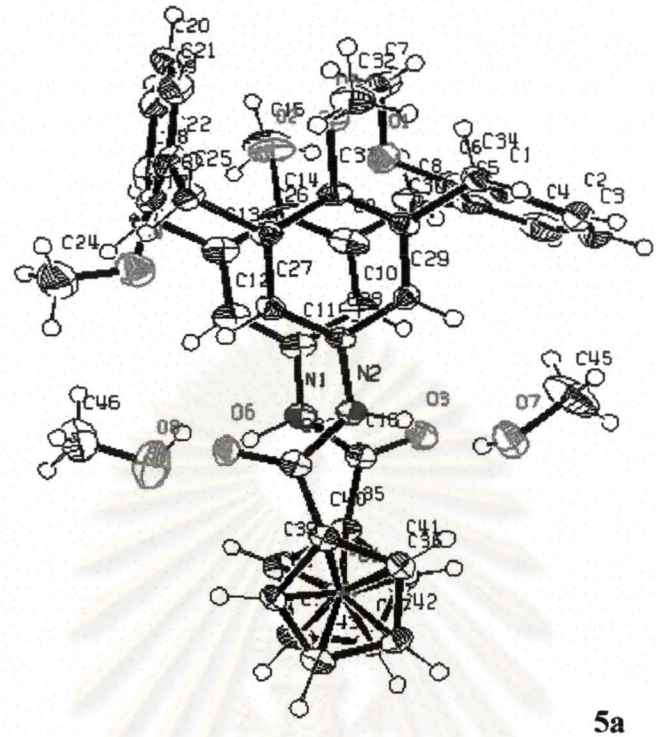

5a

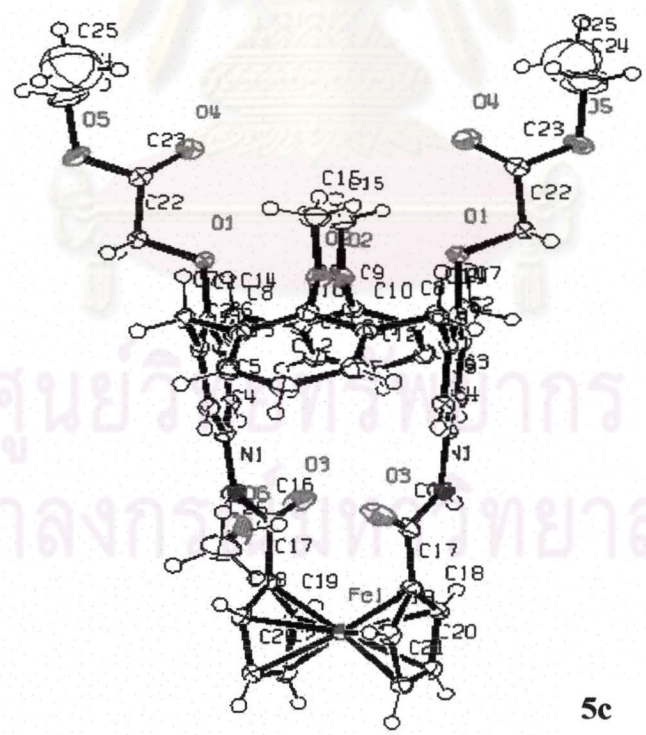

5c

Figure 3.3.13 Crystal structure of compound **5a** and **5c**

The stable structure of **5b** is in cone conformation in solid state due to the steric hindrance of 2 ethyl ester groups. As observed from x-ray structure of **5a**, one methoxy group on C7 was subjected to the anisotropic effect from inversed anisole ring. Therefore, the ^{1}H-NMR chemical shift of this methoxy group appears at high field (δ = 2.87 ppm). The molecule **5b** has one plane of symmetry between calix[4]arene rings while **5a** lacks the plane of symmetry caused by an inversed phenyl unit. Dihedral angles[101-103] between the phenyl rings and the plan of the four methylene groups are 79.17°, 75.85°, -100.83° and 24.31° for **5a** and those of **5b** are 83.97° and 35.24°. The anisole ring opposite the inversed aryl ring of **5a** is in a flattened phenyl unit attributed by the dihedral angle at 24.31° and also both unsubstituted phenyl rings of **5b** are in flatted units corresponding to dihedral angles at 35.24°. It was suggested that it is in a 'pinch cone' conformation. In the principle of calix[4]arene conformation mentioned above, cone conformation has the symmetrical C_{4v} structure while pinch cone conformation is in C_{2v} symmetry containing two opposite aromatic rings almost parallel and the other two adopted a flattened conformation.[104-105] The previous studies on the interconversion of tetra-*o*-alkylated calix[4]arene by computational study. It was predicted that a structure with C_{2v} symmetry is more stable than the more symmetrical C_{4v} structure.[99,103] Considering **5a** and **5b**, the distances between the equatorial calix[4]arene bridging methylene hydrogens (H_{eq}) and the two adjacent aromatic hydrogens (H_1, H_2 and H_3 in **chart 3.3.1**) were determined from x-ray structure identifying either the conformation is in a partial cone or a pinch cone conformation. The distance of H_{eq}-H_1 is longer than that of H_{eq}-H_2 for the pinch cone conformation. In addition, the distance of H_{eq}-H_3 is longest compared to the former distances. Undoubtedly, it was concluded that **5b** exists in a pinch cone conformation and **5a** in a partial cone conformation.[104]

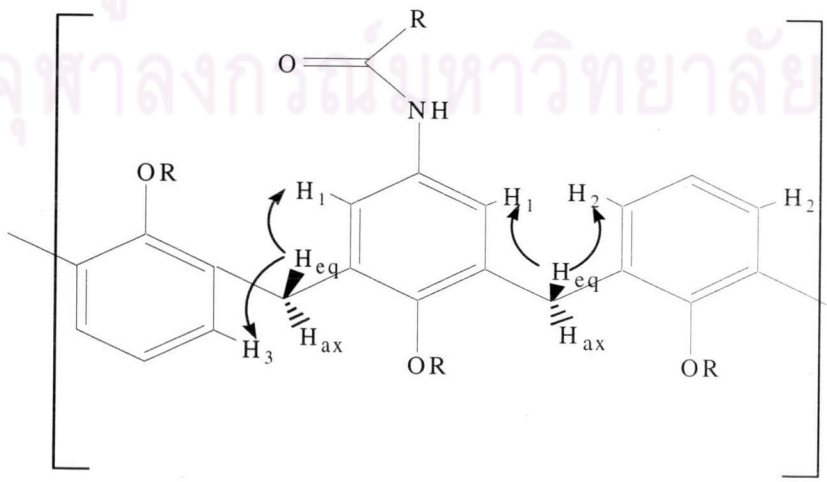

Chart 3.3.1 Correlation of proton at aromatic and methylene bridge of C and PC

Table 3.3.3 Show the distances between the H_{eq} at methylene bridge and aromatic protons.

Distance (Å)	**5a**	**5b**
H_{eq}-H_1	2.743	2.741
H_{eq}-H_2	2.348	2.421
H_{eq}-H_3	3.495	

The crystal structure of **5a** exhibited a CH_3···HC- interaction between hydrogen of methoxy groups and aromatic protons on the inversed phenyl ring with the distance around 3.425 Å which corresponds to the correlation in the NOSEY spectrum. Interestingly, the 2 oxygen atoms on amide groups point in the opposite direction when they have no interaction with guest molecules. When complexes with guests, 2 oxygen atoms on amide groups point into the same orientation. Consequently, the NH- groups were preorganized prior to bind with anion using hydrogen bonding interaction.[105] This evidence is supported by x-ray structure of bridge-cobaltocenium amide calix[4]arene.

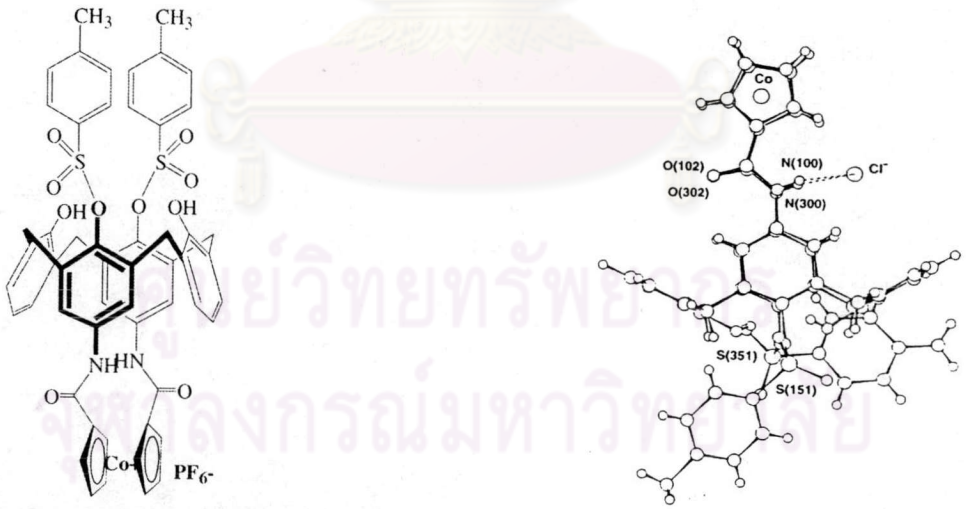

Bridge-cobaltoceniumamide calix[4]arene

Figure 3.3.14 Show crystal structure of cobaltoceniumcalix[4]arene and Cl^-

From the previous works, most ferrocene units is in the eclipsed geometry.[106-107] X-ray structures of **5a** and **5b** show the distorted eclipsed geometry of the ferrocene units possesing dihedral angles of 21.075°and 15°, respectively. For **5b**, two substituted phenyl rings is not parallel. The upper rim is tappered resualting from the ferrocene bridge.

Therefore, two diethylester groups on the lower rim point away from each other resulting in the distances of O1-O1^{i} around 5.192 Å and O4-O4^{i} around 5.782 Å while diamide ferrocene on upper rim having the distances of N1-N1^{i} and C4-C4^{i} of 4.234 Å and 4.907 Å, respectively.

Table 3.3.4 Selected Bond Distances (Å) and Angles (deg) for **5a**

O1-C6	1.376(5)	N1-C11	1.428(5)	Fe1-C39	2.053(4)
O1-C7	1.448(5)	N1-C16	1.361(6)	C1-C34	1.523(6)
O2-C14	1.398(5)	N1-H1N	1.12(4)	C5-C8	1.507(8)
O2-C15	1.437(5)	N2-C28	1.429(5)	C8-C9	1.522(7)
O3-C16	1.225(5)	N2-C33	1.369(5)	C13-C17	1.505(7)
O4-C23	1.396(5)	N2-H2N	0.96(6)	C16-C35	1.490(6)
O4-C24	1.390(5)	Fe1-C35	2.043(4)	C33-C40	1.482(6)
O5-C31	1.385(4)	Fe1-C36	2.053(4)	C17-C18	1.511(7)
O5-C32	1.436(5)	Fe1-C37	2.061(4)	C22-C25	1.463(6)
O6-C33	1.234(5)	Fe1-C38	2.059(4)	C25-C26	1.513(6)
				C30-C34	1.526(5)
C6-C1-C34	120.2(4)	N1-C16-C35	115.6(3)	C27-C28-N2	124.2(3)
C2-C1-C34	122.0(4)	C13-C17-C18	110.5(3)	C29-C28-N2	115.6(3)
C5-C8-C9	112.6(4)	C13-C17-H17A	109.6	C31-C30-C34	121.3(3)
C5-C8-H8A	109.1	H17A-C17-H17B	108.1	O6-C33-N2	123.3(3)
H8A-C8-H8B	107.8	C23-C18-C17	121.6(4)	N2-C33-C40	115.3(3)
C14-C9-C8	123.0(4)	C19-C18-C17	120.7(4)	C30-C34-C1	110.6(3)
C10-C9-C8	117.9(4)	C23-C22-C25	120.8(4)	C30-C34-A34A	109.5
C10-C11-N2	123.6(4)	C21-C22-C25	122.5(4)	H34A-C34-H34B	108.1
C12-C11-N1	116.1(4)	C22-C25-C26	109.4(3)	C16-C35-Fe1	126.6(3)
C12-C13-C17	121.1(4)	C22-C25-H25A	109.8	C41-C40-C33	131.6(4)
C14-C13-C17	122.1(4)	H25A-C25-H25B	108.3	C44-C40-C33	121.8(4)
O3-C16-N1	124.2(4)	C31-C26-C25	119.6(3)	C16-N1-C11	127.4(4)
O3-C16-C35	120.1(4)	C27-C26-C25	120.6(3)	C16-N1-H1N	115(2)
C11-N1-H1N	116(2)	C40-Fe1-C44	41.49	C40-Fe1-C42	68.24(7)
C33-N2-C28	127.3(3)	C40-Fe1- C35	112.4(3)	C40-Fe1-C37	171.57(19)
C33-N2-H2N	124(3)	C40-Fe1-C36	134.35	C40-Fe1-C38	148.68(17)
C28-N2-H2N	108(3)	C40-Fe1-C39	118.12		

Table 3.3.5 Selected Bond Distances (Å) and Angles (deg) for **5c**

O1-C1	1.400(3)	O4-C23	1.195(4)	N1-C4	1.418(3)
O1-C22	1.414(3)	O5-C23	1.341(4)	N1-C16	1.350(4)
O2-C9	1.380(3)	O5-C24	1.436(5)	N1-H1	0.760(4)
O2-C13	1.428(4)	O6-C26	1.401(4)	Fe1-C17	2.046
O3-C16	1.235(4)	O6-H6	0.8400		
C3-C2-C7	118.0(2)	C8-C7-H7A	109.7	C18-C17-C16	129.6(3)
C1-C2-C7	122.4(2)	H7A-C7-H7B	108.2	C21-C17-Fe1	69.57(16)
C5-C4-N1	118.1(2)	O2-C9-C8	119.1(2)	C16-C17-Fe1	127.3(2)
C3-C4-N1	122.3(2)	C12-C15-C14^{i}	122.4	O1-C22-C23	108.8(2)
C1-C6-C14	122.3(2)	O3-C16-N1	123.3(3)	O4-C23-O5	124.5(3)
C5-C6-C14	118.9(2)	O3-C16-C17	120.6(3)	O4-C23-C22	126.6(3)
C8-C7-C2	109.7(2)	C21-C17-C16	122.3(3)	O5-C23-C22	108.9(3)

3.3.2 Binding properties of 5a, 5b and 5c towards anions and cations

3.3.2.1 Binding properties with anions for 5a, 5b and 5c

In the past decade, many artificial molecules were synthesized for binding anions. There are 2 types of anion receptors: charged receptors and neutral receptors. Charged receptors are –NH- group or ammonium[108-110], guanidinium and amidinium[111-112], as well as pyridinium.[113] Neutral receptors possess calixpyrroles[114-115], amide (-CONH-)[116-117] and thiourea (-NHCSNH-) or urea (-NHCONH-)[118-119] for binding anions. Our molecules consist of both anion and cation binding sites. Compounds **5a**, **5b** and **5c** containing CONH group as hydrogen bond donor were subjected to study their ability to bind various shapes and charges of anions such as spherical geometry (Cl^-, Br^- and I^-), planar or Y-shape (NO_3^-, CH_3COO^- and $C_6H_5COO^-$) and tetrahedral geometry ($H_2PO_4^-$, HSO_4^-). In addition, compounds **5b** and **5c** have the ethyl ester groups (for binding cation), attached on the lower rim of calix[4]arene. We would like to study the effect of cations to anion binding properties of **5b** and **5c**. The recognition of three ligands with tetrabutylammonium salts, Cl^-, Br^-, I^-, NO_3^-, HSO_4^-, $H_2PO_4^-$, acetate and benzoate, was measured by ^{1}H-NMR titrations. Firstly, binding studies of three ligands were carried out in $CDCl_3$. Interestingly, the ratio of cone to partial cone conformation of **5a** in $CDCl_3$ changes upon addition of Cl^- and $H_2PO_4^-$. From the integration of signals of Cp ring

protons, we can estimate the ratios of cone and partial cone conformation as shown in **Table 3.3.6** The results implies that **5a** can recognize Cl^- and $H_2PO_4^-$ by changing its conformation. Due to the unconformity of the ratio of cone and partial cone conformation of **5a** during anion titration, vide infra, the stability constants of **5a** toward anions, however, cannot be estimated.

Table 3.3.6 Mole fraction (X) of cone (C) and partial cone (PC) conformation when increasing the ratio of anion to **5a**

Anion	X_c/X_{pc} with various **5a** : anions ratios		
	1:0	1:1	1:4
Cl^-	0.452/0.548	0.427/0.573	0.395/0.605
$H_2PO_4^-$	0.452/0.548	0.448/0.552	0.427/0.573

The association constants depend on the solvent system. The acceptor number (AN) of solvents should be realized in term of anion recognition. Solvents that have the high acceptor number (AN) will have the high affinity for anionic species. Consequently, the ability of receptors to complex anion decreased. The acceptor numbers of $CHCl_3$ and CD_3CN are 23.1 and 12.5, respectively.[120] The K values of complexes measured in $CDCl_3$ are very low. We, therefore, measure binding constants of compounds **5a**, **5b** and **5c** with anions in CD_3CN. The binding constants of **5a**, **5b** and **5c** were carried out by ^{1}H-NMR titration upon the addition of anion guest molecules at room temperature. The ^{1}H-NMR spectra were recorded until no peak shift appeared upon adding anions. The titration curves between **5a**, **5b** and **5c** with acetate are shown in **Figure 3.3.15**

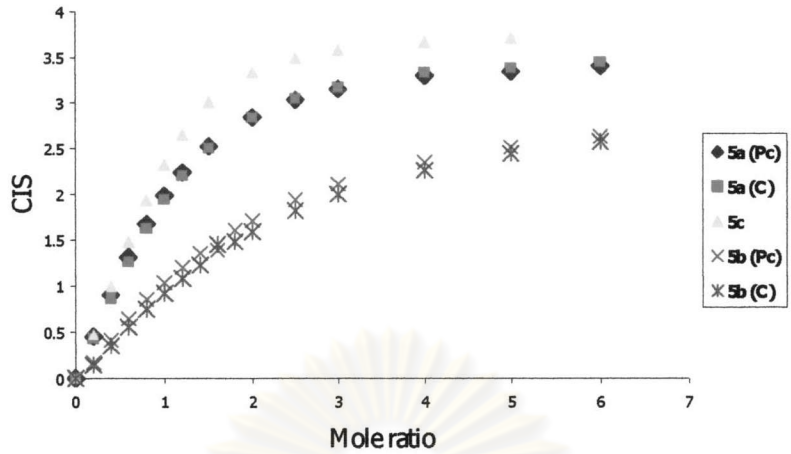

Figure 3.3.15 Titration curves between **5a**, **5b** and **5c** with acetate in CD_3CN

And the titration curves between **5a** with various anions are shown in **Figure 3.3.16**

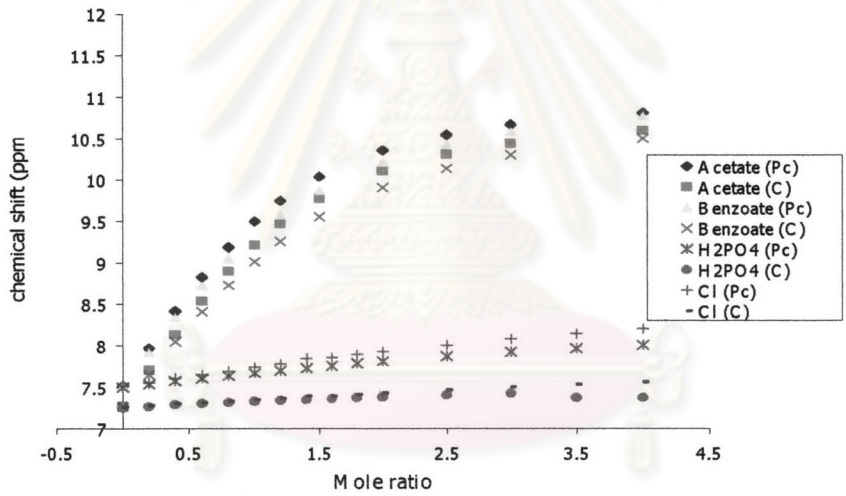

Figure 3.3.16 Titration curves between **5a** and various anions in CD_3CN

Curve **5c** exhibited larger chemical shift than other ligands. These behaviors implies a high stability constant. The titration curves display the 1:1 stoichiometry. Obviously, titration curves between compound **5a** and various anions show that in the large shifts occur for carboxylate anion but smaller shifts for $H_2PO_4^-$ and Cl^-. Compounds **5a**, **5b** and **5c** possessing the amide NH groups forming a bi-dentate hydrogen bonding array that are complementary to carboxylate anions and $H_2PO_4^-$. Therefore, halide anions give smaller K values. However, all ligands give a slight shift for $H_2PO_4^-$ comparing to carboxylate anion due to the low basicity of $H_2PO_4^-$.[121] The stability constants of compounds **5a**, **5b** and **5c** are summarized in **Table 3.3.7**.

Table 3.3.7 The stability constants of compound **5a**, **5b** and **5c** toward various anions at room temperature in CD_3CN-d^3 (M^{-1})

Anions	5a		5c		5b
	PC	C	PC	C	C
$PhCOO^-$	540	472	139	100	915
CH_3COO^-	826	741	227	174	1200
$H_2PO_4^-$	34	a	91	94	a
Cl^-	32	a	49	86	29

PC = partial cone conformation ; C = cone conformation

a, K values could not refined.

All association constants have errors less than 10%.

As mentioned previously, compounds **5a** and **5b** exist in cone and partial cone conformation in solution at room temperature. Two different N*H* signals were observed at 8.09 and 7.86 ppm for **5a** and at 8.10 and 7.88 ppm for **5b** belonging to partial cone conformation and cone conformation, respectively. In CD_3CN, both cone and partial cone conformations ratios of **5a** and **5b** are constant. K values showed that all compounds in cone and partial cone conformations preferably formed with acetate anion. Unfortunately, all ligands have no interaction with Br^-, I^-, NO_3^- and HSO_4^- observing from no NH signal shifts upon addition of these anions possibly due to unmatched size or charge density of anions. In the case of HSO_4^-, it can preferentially bind with molecules containing a basic amine functionality because the acidic hydrogen sulfate ion is capable of protonation the amine groups and the positively charged receptor strongly binds the produced SO_4^-.[121] Futhermore, all ligands bind preferentially with acetate over benzoate due to the basicity order of acetate and benzoate.[121] Plots of chemical shift (*vide supra*) between **5a**, **5b** as well as **5c** and acetate signified the high K values. Anion binding constants of compounds **5a** and **5b** of partial cone conformation are superior to those of cone conformation. All ligands give the favorite to anions in a Y-shape geometry.

especially acetate and benzoate. The association constants with anions are in order of **5c** > **5a** > **5b**. All ligands selectively bind carboxylate over halide anions and $H_2PO_4^-$. The previous works of Beer and coworkers[123-124] studied the association constants of the molecules containing cobaltocenium at the upper rim of calix[4]arene. The anion-coordination properties of cobaltocenium bridge calix[4]arene receptors are dependent upon the degree of preorganization of the upper rim.

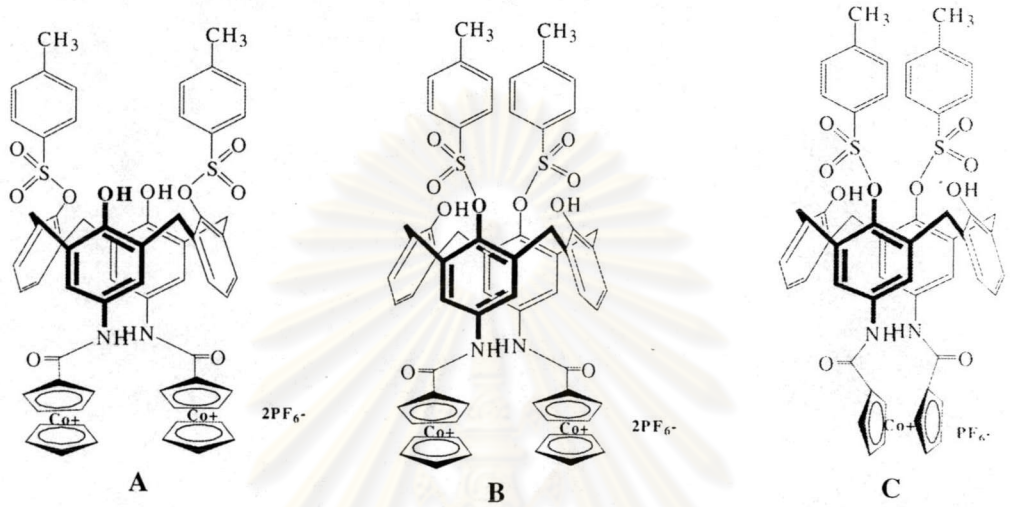

Figure 3.3.17 Calix[4]arenes contain cobaltocenium and tosyl groups

It was found that the position of tosyl substituent on lower rim of calix[4]arene has a dramatic influence on the anion coordination properties of upper rim. For instances, compound **A** binds with acetate much better than $H_2PO_4^-$, whereas the selective preference is reversed with an isomeric **B**. In the case of compound **C**, it formed thermodynamically stronger anions complexes with carboxylate than either compound **A** or **B**, and with a notable selectivity for acetate. The electron withdrawing tosyl-substituents at the *para* position on phenyl group bearing amide moieties induced the increasing in acidity of the NH protons and resulted in the higher affinity for acetate which is more basic than $H_2PO_4^-$. (pK_a of $CH_3COOH = 1.7x10^{-7}$, pK_a of $H_3PO_4 = 7.1x10^{-3}$).[125] It is the worthwhile to point out why the association constants of **5a**, **5b** and **5c** with carboxylate anions are much higher than other anions due to the substituent groups on lower rim. However, the predicted association constants with acetate should be in order of **5c**, **5b** and **5a**. Receptor **5b** and **5c** posses the electron withdrawing ethyl ester substituents at *para* position on phenyl units with amide groups. However, **5c** has more affinity for anions comparing to **5b** since **5c** is rigidified from four ethyl ester bulky groups to give a high degree of preorganization.[126] In contrast, **5a** has the electron

donating methoxy group at the anisole rings bearing amide groups. This is the reason that it displays lower anion recognition than **5c** related the K values but higher binding ability than **5b**. Presumably, the effect of water in the deuterated solvent competed the binding with anions.[125] Water is competitive to bind with NH using hydrogen bonding interaction resulting in less K values of complexes between host and guest molecules even the traces of water in deuterated solvent. The higher intensity of water signals was observed in titration spectra of **5b** due to moisture. Predictable formation between amide calix[4] arene and acetate was related to the work's Beer.[70] The structure of bridge-cobaltocenium amide calix[4]rene are similar to our compounds and therefore, the complexes with carboxylate should have a similar structure. The proposed structure is shown in **Figure 3.3.18**.

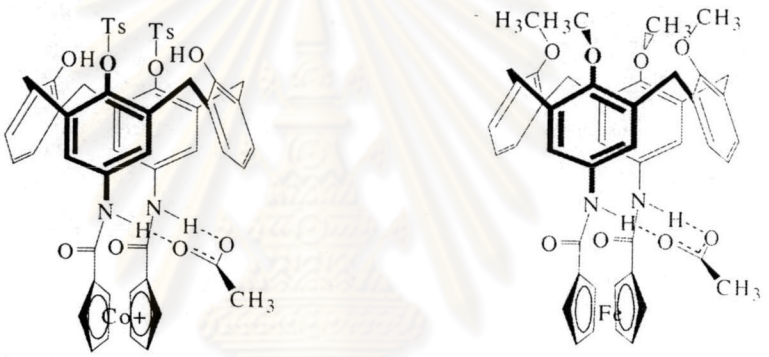

Bridg-cobalttocenium calix[4]arene **5a**

Figure 3.3.18 The proposed structure of complex between bridge-ferrocene amide calix [4]arene and acetate

Additionally, aromatic signals in ^{1}H-NMR spectra of titration between **5a** with benzoate significantly shifted as shown in **Table 3.3.8**.

Table 3.3.8 Chemical shift of complex between **5a** and Benzoate

Ratio of Ligand:anions	0.0	1.0	1.5	2.0	Δδ
NH (PC)	7.515	9.321	9.865	10.207	2.692
NH (C)	7.267	9.008	9.552	9.905	2.638
m-Ar*H*OCH$_3$ (C) d, *J* = 7.8 Hz	7.254	7.121	7.083	7.059	-0.195
m-Ar*H*OCH$_3$ (PC) d, *J* = 7.2 Hz	7.141	7.093	7.073	7.059	-0.082
p-Ar*H*OCH$_3$ (C) t, *J* = 6.9 Hz	7.054	6.720	6.609	6.547	-0.507
p-Ar*H*OCH$_3$ (PC) t, *J* = 6.9 Hz	6.977	6.834	6.805	6.764	-0.213
o-Ar*H*NHCO (PC)	6.559	6.801	6.874	6.918	0.359
o-Ar*H*NHCO (C)	6.428	6.566	6.609	6.637	0.209
o-Cp*H*CONH (PC)	4.928, 4.836	5.229, 4.916	5.317, 4.935	5.379, 4.947	0.451, 0.111
o-Cp*H*CONH (C)	4.755	4.945	5.004	5.042	0.287

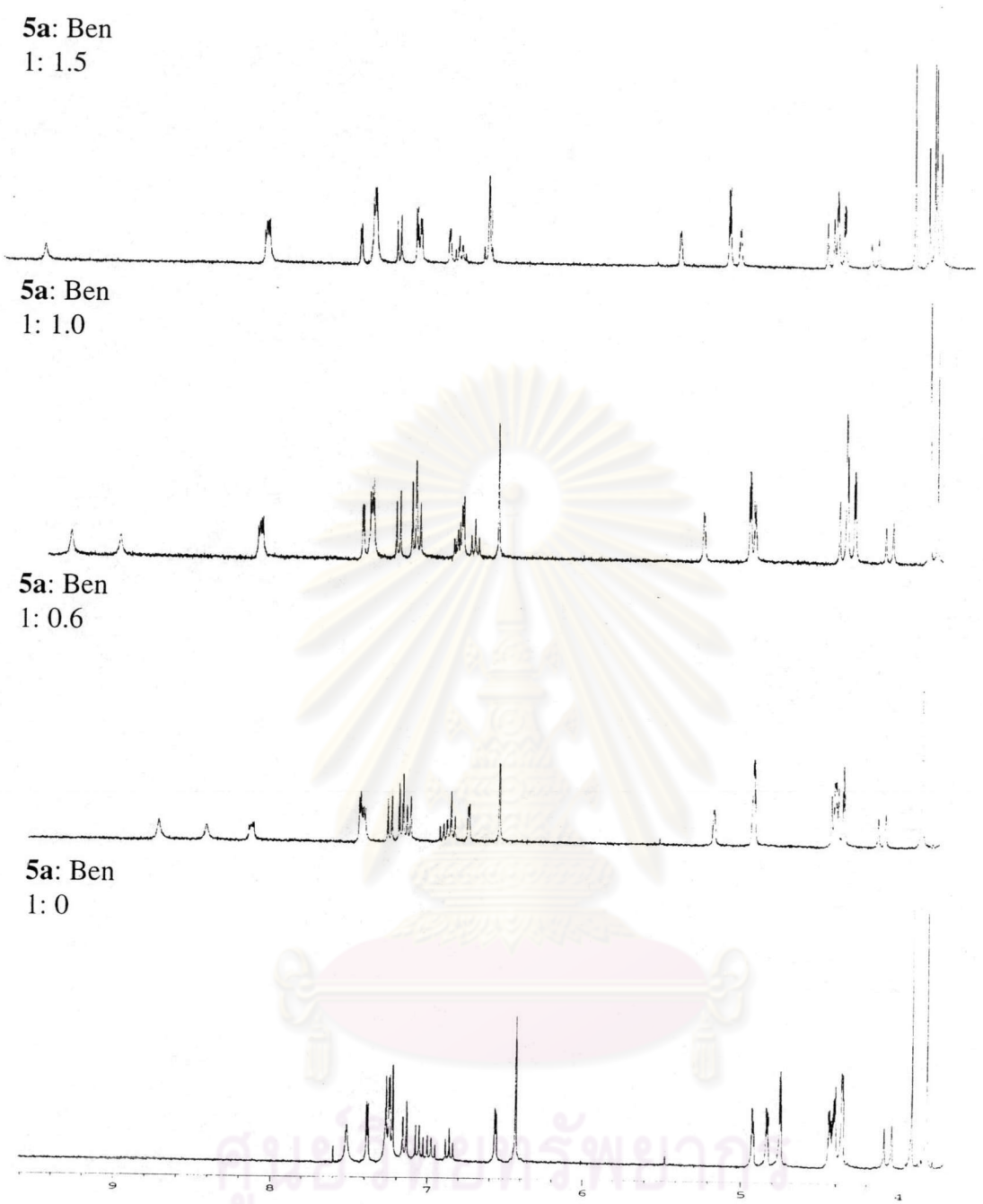

Figure 3.3.19 ^{1}H-NMR spectrum of **5a** and Benzoate in CD_3CN with 400 MHz

It is noteworthy that the complexes give the influence on aromatic rings of receptors. This behavior is possibly similar to the previous work. Cameron and Loeb[126] have synthesized calix[4]arene derivatives containing amide group with different number of electron withdrawing chloro-substituents at 1 and 3 position of upper rim. It was found that these receptors could bind strongly with benzoate. The formation is attributed to the calixarene adopting a 'pinched cone' conformation resulting in not only the two amide

groups becoming parallel but also one phenyl ring of calix[4]arene is parallel to benzoate ring.

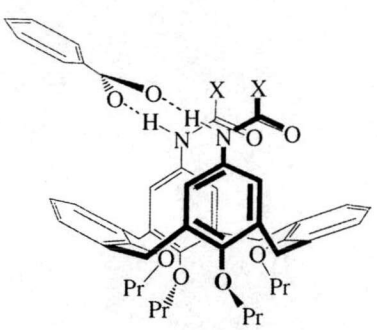

I X = CH_2Cl
II X = $CHCl_2$
III X = CCl_3

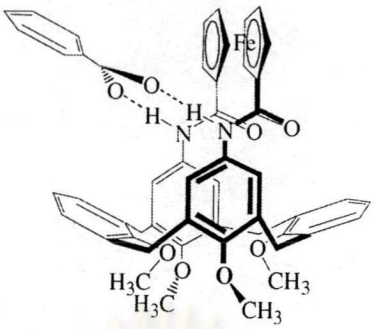

5a (C) and benzoate

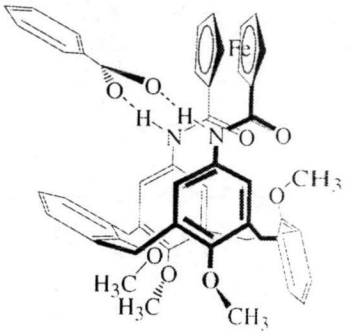

5a (Pc) and benzoate

Figure 3.3.20 The proposed structure of complex with benzoate

This phenomenon is analogous to **5b** and **5c** as shown in **Figure 3.3.21 and 3.3.22**. Elucidation by NMR spectra for PC signals indicates that aromatic protons of the non-inversed phenyl ring showed larger shifts over those of the inversed phenyl ring. The results are obtained by the ring current effect from benzoate. For the instances, protons of *p*-Ar*H*OCH_3 (PC) pointed into the ring current and shifted to more upfield. On the other hand, protons of *o*-Ar*H*NHCO- (PC) appeared more downfield because they are outside the ring current from the non-inversed phenyl ring of the building block. The downfield shift of the Cp*H* protons took place significantly by means of the effect of hydrogen bond interaction between NH--$^{-}OOCC_6H_5$. The proposed structure is shown in **Chart 3.3.2**.

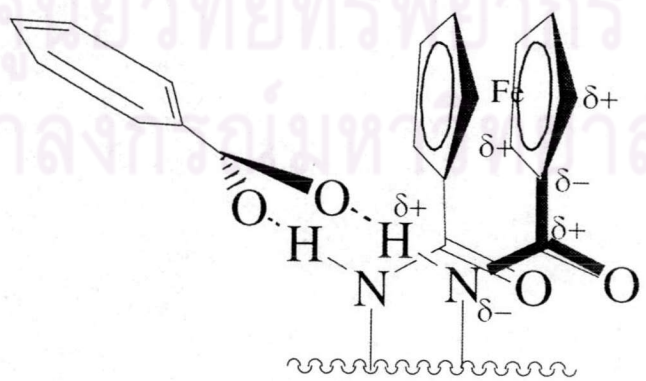

Chart 3.3.2 Show the effect of hydrogen bond interaction on Cp*H* signals

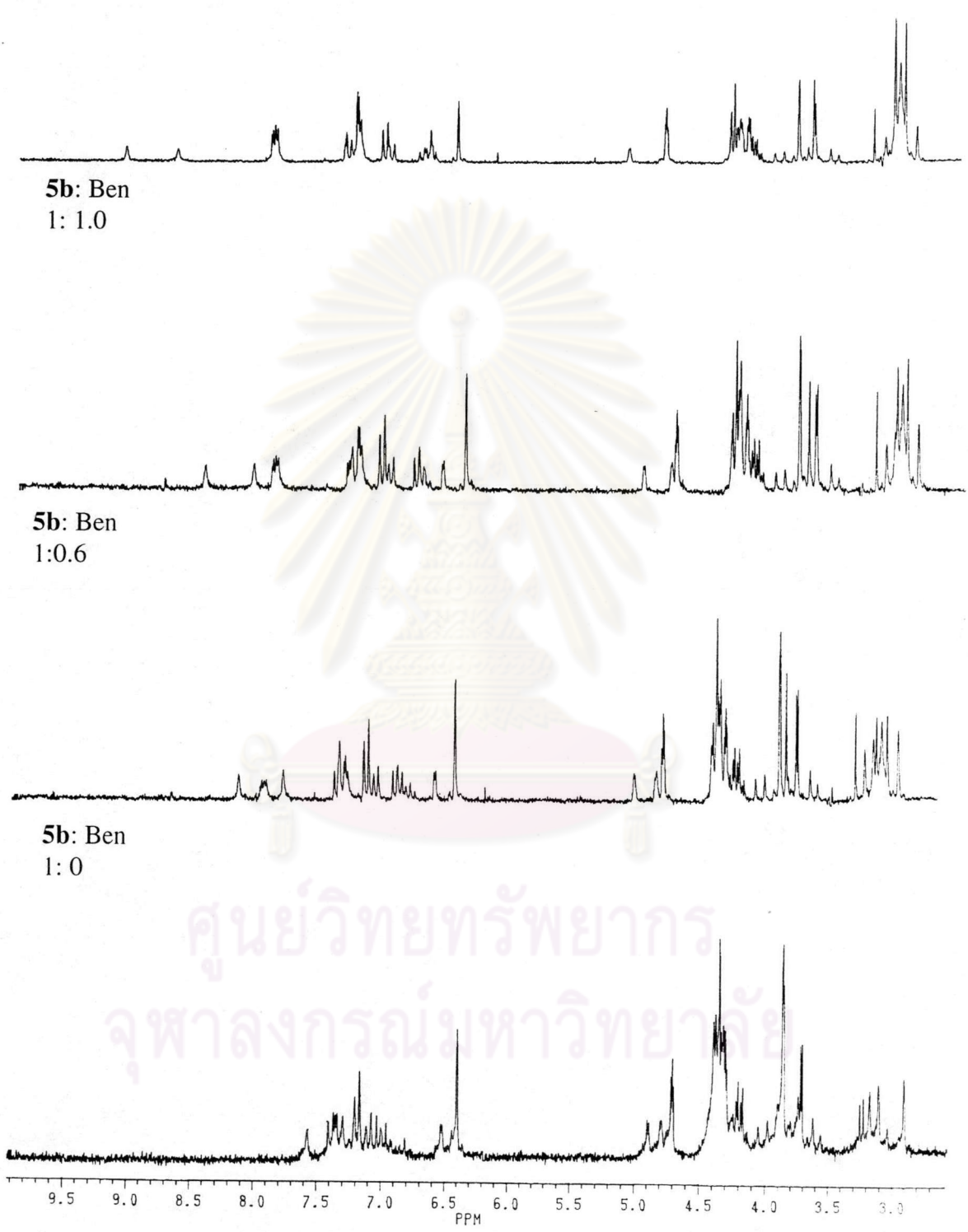

Figure 3.3.21 ^{1}H-NMR spectrum of **5b** and Benzoate in CD_3CN with 200 MHz

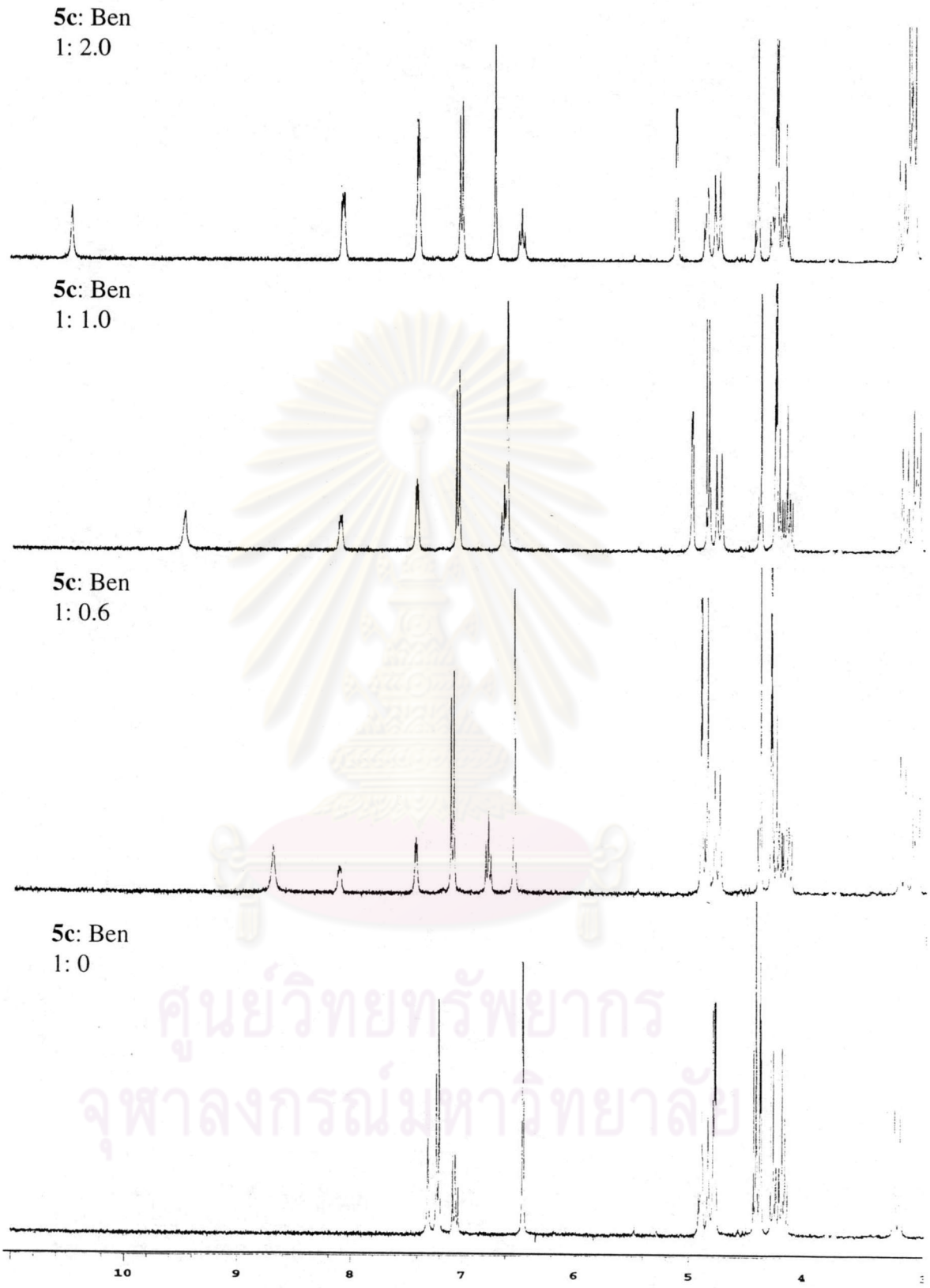

Figure 3.3.22 ^{1}H-NMR spectrum of **5c** and Benzoate in CD_3CN with 300 MHz

We took attempts to grow single crystals of these complexes but unfortunately, the complexes decomposed whilst they were left in solution over 3 days. Furthermore, the NOESY and ROESY of these complexes were carried but no more data supported the assumption according to no cross peak correlation observed clearly in the spectra.

3.3.2.2 Binding properties of cations with 5b and 5c

As mentioned above, the designed molecules consist of 2 binding sites, one for anion recognition from amide moieties and the other for cation recognition from ethyl ester groups. Compounds **5b** and **5c** contain the ethyl ester groups, which are able to bind alkaline metals.[127-129] The difference between both ligands is the number of ethyl ester groups. The points of study are to compare the affinity for cation and the effects of cation binding towards anion binding strength. Previously, the simultaneous complexation of cation and anion guest species by bifunctional receptors were studied and found that the presence of cation enhanced the anionic binding abilities in terms of ion-pair recognition.[130-135] Recently, many ditopic receptors employed the calix[4]arene as building block. These receptors were classified into two types: cation and anion binding sites are in the same side of calix[4]arene and both binding sites are in the opposite side of the building block. Basically, the anion binding constants were enhanced significantly from cation binding in the case of ditopic receptors which have cation binding and aion binding sites in the same side of the framework. Beer and co-workers[137] studied the simultaneous stability constant of cations and anions. Their compounds were shon in **Figure 3.3.23**. The simultaneous co-ordination of a cation and an anion is at the benzo crown amide substituted at the lower rim of calix[4]arene.

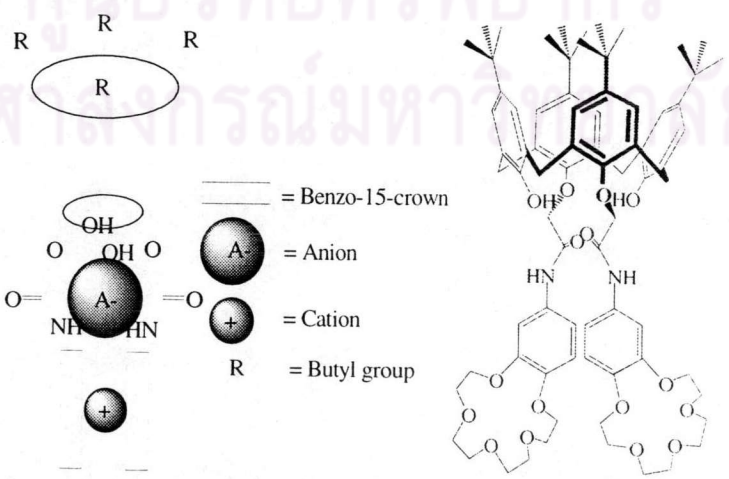

Figure 3.3.23 Show the ditopic receptor for both cationic and anionic species

They suggested that the K values of this ligand with K^+ ion and either $H_2PO_4^-$ or HSO_4^- are much higher compared to those of ligand without K^+. The electrostatic interaction of the ion-pair is directly attributable the complexation. Our receptors have the cation binding site at the lower rim and the anion binding site at the upper rim. The binding enhancement occurred from the effect of cation through phenyl bonds and ion-paired enhancement.

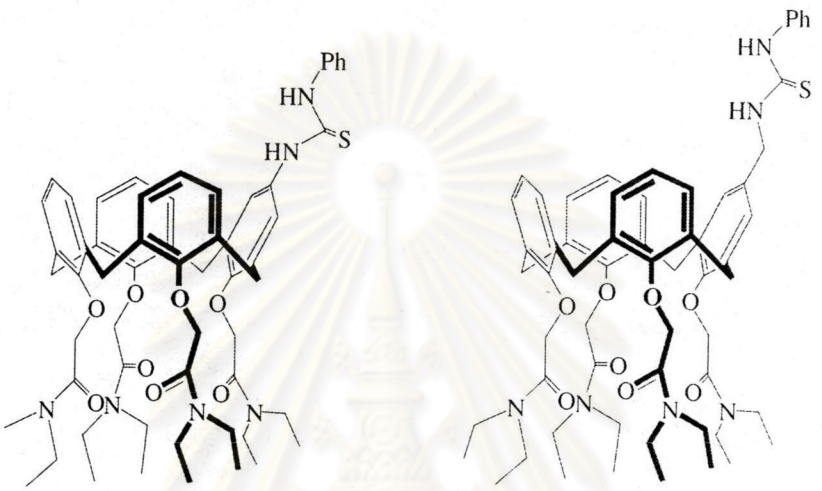

A **B**

Figure 3.3.24 Show the ditopic receptors having cation and anion binding sites not the same side

Ungaro and co-workers[63] designed ligands **A** and **B** in order to compare their binding enhancements due to the simultaneous binding with cations and anions. The anionic association constant indicated that receptor **A** with K^+ increased the K values. On the other hand, this behavior is reversed with receptor **B**. It was assumed that the urea group at the upper rim for receptor B obtained a little effect of the amide group at the lower rim due to a CH_2 spacer. Our receptors containing ethyl ester moieties were expected to bind with alkali metals and to give the influence on anion binding properties. The methodology of study the effect of cation complexation on anion binding is the preparation of the saturated cation binding site by adding one equivalent of alkali salts and then the association constants with anions were evaluated by adding variable amounts of tetrabutylammonium salts (TBA). The titration experiments were recorded by ^{1}H-NMR spectrometer. Unfortunately, no signals shift under complexes with alkali salts. Moreover, the results of ^{1}H-NMR spectra show no peaks shift during adding the amount

of tetraammonium salt. Upon adding more anion salts, not only NH signal shifted gradually but also the precipitate was observed in on NMR tube. It suggested that **5c** have ability to bind weakly to alkali metals (Na^+ and K^+). The metal ion is labile and forms salt with added anion. Therefore, we cannot evaluate the stability constants for the complexes of ligand with metal and anion guests. We presumed that the upper rims were rigidified by ferrocene bridge which locks the position of the aryl rings and the ethyl ester groups at lower rims are too far apart to form comples with cation. (**Figure 3.3.25**)

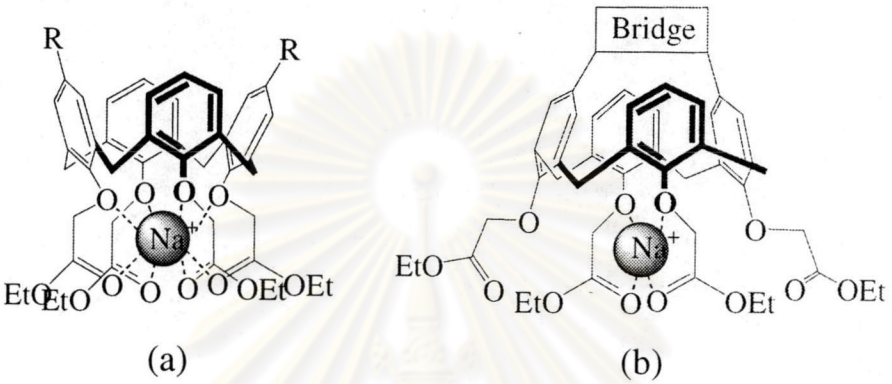

Figure 3.3.25 Proposed Na^+ cation binding for calix[4]arene tetraethylester derivatived : (a) normal Na^+ binding (b) lower rim binding site disrupted by the upper rim bridge.

The distances between 2 ethyl ester groups on the substituted aryl rings were mentioned in x-ray part. The rest of ethyl ester groups on the unsubstituted aromatic rings are capable of binding with cation with weak interactions in the case of **5c** but not for **5b.** These are the reason of the precipitation of sodium or potassium states upon addition of anion. Similarly, Reinhoudt and co-workers[138] studied the bifunctional receptors containing the urea moieties at upper rim and tetraethyl ester at lower rim of calix[4]arene.

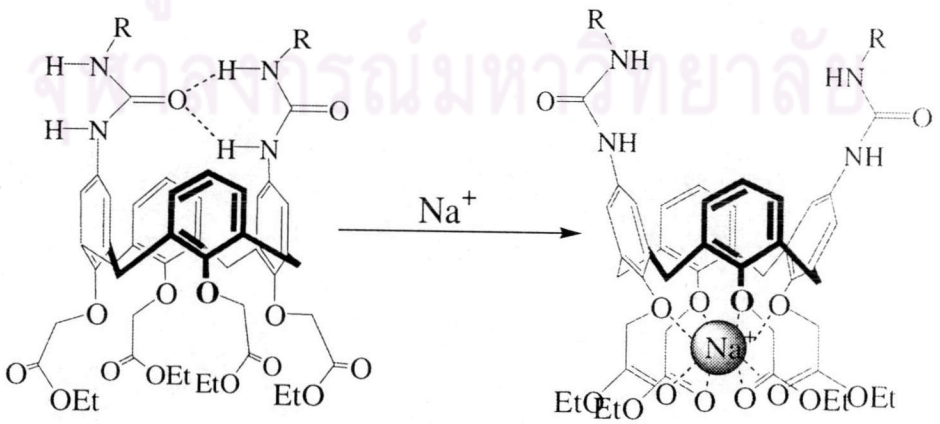

Figure 3.3.26 Complexation of Na^+ ions with ditopic receptor

This ligand cannot bind with anion in the absence of Na^+ since the intramolecular hydrogen bond interaction of urea moiety blocks anionic molecules. In the presence of Na^+ cation, four ethyl ester groups can adjust themselves to bind Na^+ ions and destroy the hydrogen bond interaction of the urea groups. Unrigidified molecule is able to bound with anions. Unlike **5c**, due to the ferrocene bridge, ethyl ester groups cannot be rearranged in a suitable orientation for binding cations. However, the weak binding of metal by the ligand can be determined by electrospray ionization mass spectrometry.

Mass Spectroscopy. ESI-MS $C_{56}H_{56}O_{14}N_2Fe$ = 1036.31 [M, 1036.91]

$C_{56}H_{56}O_{14}N_2FeNa$ = 1059.90 [M+Na]

$C_{56}H_{56}O_{14}N_2FeK$ = 1076.00 [M+K]

$C_{56}H_{56}O_{14}N_2FeRb$ = 1122.39 [M,+Rb]

$C_{56}H_{56}O_{14}N_2FeCs$ = 1169.81 [M+Cs]

The results of mass spectrometry displayed the major peak of **5c** with Na^+ but the rest of alkali metals showed only small peaks. It is assumed that **5c** binds selectively with Na^+ according to the hard-soft acid-base principle. The ethyl ester groups have oxygen donor atoms as hard bases which prefer to form complex with hard acids such as Na^+.[139]

3.3.2.3 Electrochemical studies

As mentioned above, three ligands, **5a**, **5b** and **5c** contain ferrocene units at the upper rim of the calix[4]arene building block. Naturally, ferrocene unit has ability to display the electrochemical signal. Therefore, the electrochemical properties of these ligands can be studied by techniques such as cyclic voltammetry and square wave voltammetry. The cyclic voltammetry and the square wave techniques were performed using solutions of **5a**, **5b** and **5c** (**1** x 10^{-3} M) in distilled anhydrous acetonitrile with 0.1 M Bu_4NPF_6 as supporting electrolyte and using a glassy carbon working electrode, a Ag/Ag^+ reference electrode and a Pt wire counter electrode. All solutions were purged with N_2 before measurements. The potential was scanned in the range of 0.15 to 0.55 V

at 50 mV/s. The cyclic voltammograms of **5a**, **5b** and **5c** give reversibly redox couples as shown in the **Figure 3.3.27**. The values of the potential for the redox couples were shown in **Table 3.3.9**.

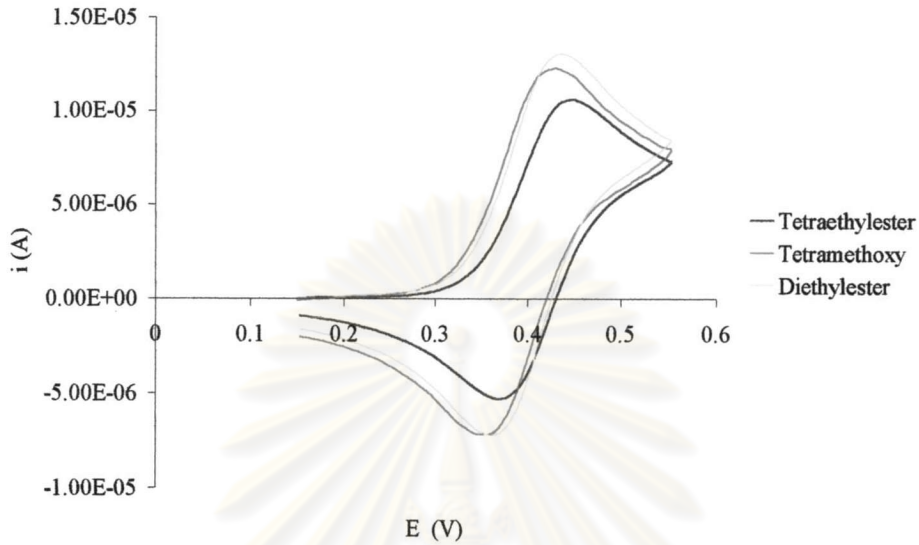

Figure 3.3.27 Cyclic voltammograms of **5a**, **5b** and **5c** in acetonitrile with 0.1 M TBAPF

Table 3.3.9 The characteristic values of **5a**, **5b** and **5c**

Ligands	E_{pa} (V)	E_{pc} (V)	$E_{1/2}$	ΔE (V)	I_{pa}/I_{pc}
5a	0.412	0.354	0.383	0.058	1.01
5b	0.428	0.370	0.399	0.058	1.02
5c	0.448	0.385	0.414	0.058	1.02

All CVs measurements of the free ligands were carried out by varied scan rates at 20, 50, 80, 100, 200, 500, 800 and 1000 mV/s. Cyclic voltammograms of **5a**, **5b** and **5c** at various scan rates in acetonitrile are depicted in **Figure 3.3.28**. The correlation between current (i) and square root of scan rates ($v^{1/2}$) was plotted and shown in **Figure 3.3.29**.

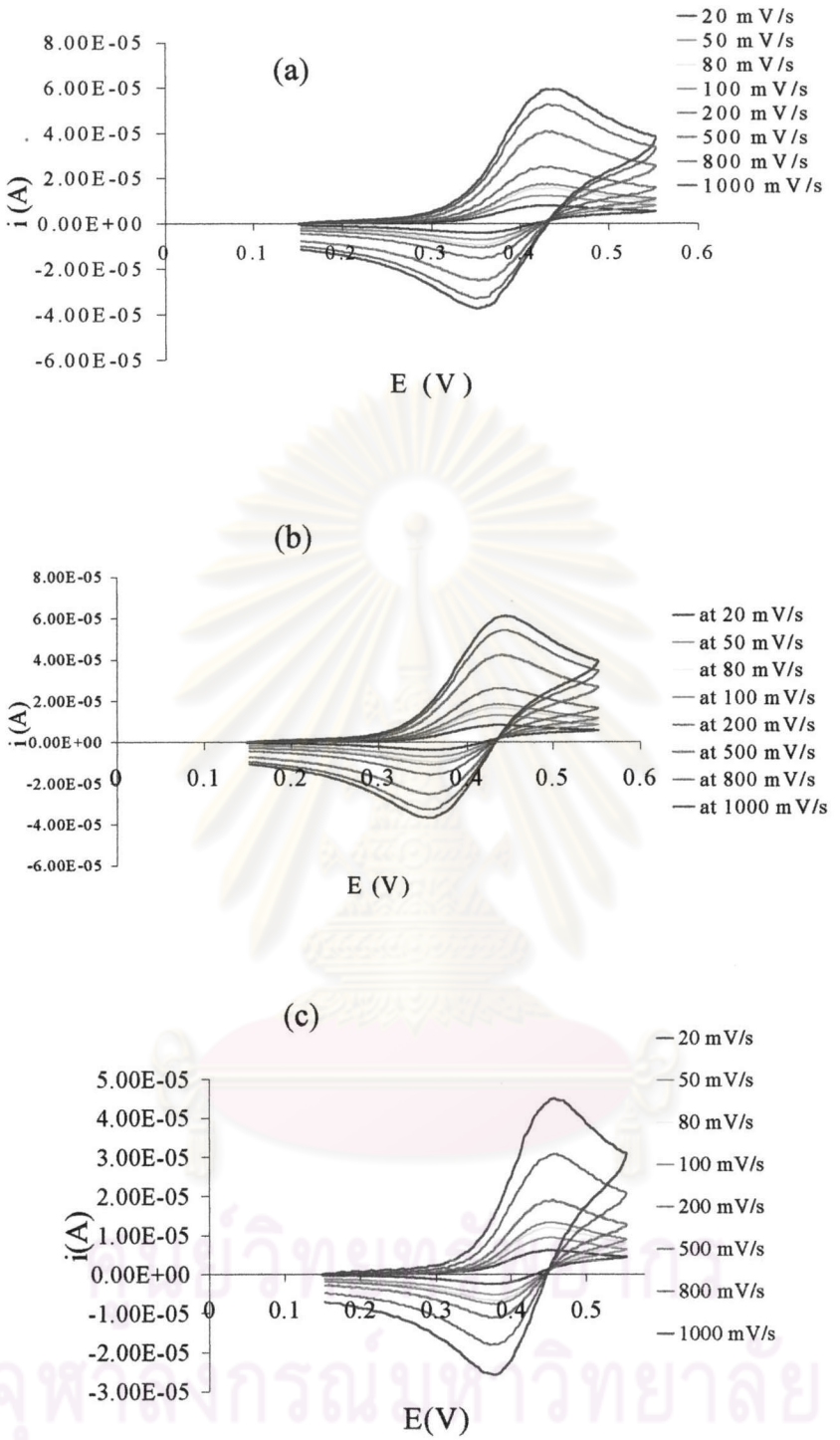

Figure 3.3.28 Cyclic voltammograms of **5a** (a) **5b** (b) and **5c** (c) in acetonitrile with 0.1 M TBAPF at different scan rates

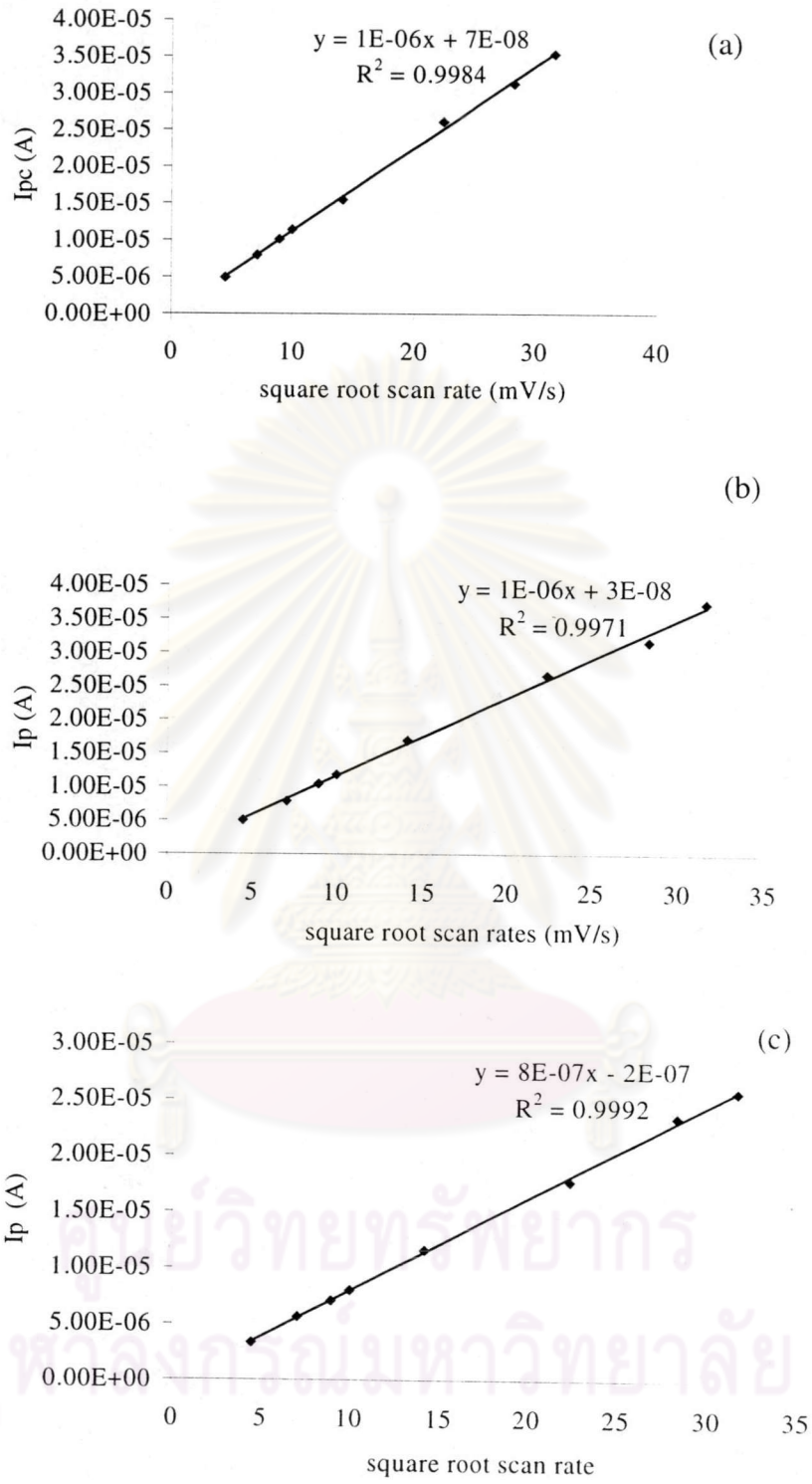

Figure 3.3.29 Plots of currents and square root of scan rates ($\nu^{1/2}$) for **5a** (a) **5b** (b) and **5c** (c)

All ligands have the anodic and cathodic intensities ratios close to the unity and the ΔE is equal to 58 mV corresponding to a one electron transfer process. The plot of i_p and $\nu^{1/2}$ is

a straight line passing though the origin. This indicates that i_p is proportional to $v^{1/2}$, a characteristic of the reversible electron transfer. The redox couples of **5a**, **5b** and **5c** are conceptually reversible system of Fe^{II}/Fe^{III} redox centers. Additionally, the proportion of i_p and $v^{1/2}$ displays the diffusion system. Interestingly, in the case of potentials carried out in the range of 0.15 – 1.25 V, another irreversible peak appeared at the potential range of 0.85-1.22 V. It was the one-electron electrochemical oxidation of aryl ether units of calix [4]arene.[140-141] (**Figure 3.3.30**)

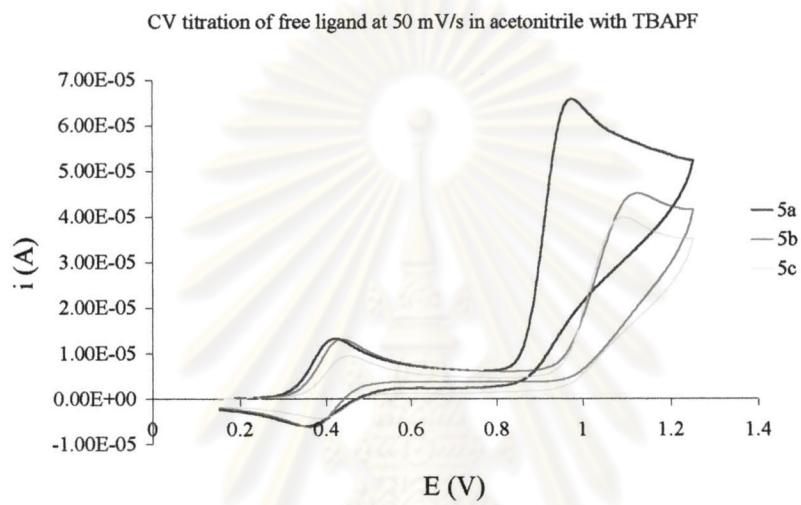

Figure 3.3.30 Cyclic voltammograms of **5a**, **5b** and **5c** at 50 mV/s in acetonitrile with 0.1 M TBAPF

The ethyl ester substituents on hydroxy oxygens are electron withdrawing groups and destabilize the positive charge of the oxidized oxygen atom as shown in **Figure 3.3.31** It is thus support the higher oxidation potential for **5b** and **5c** compared to **5a** bearing the methoxy groups.

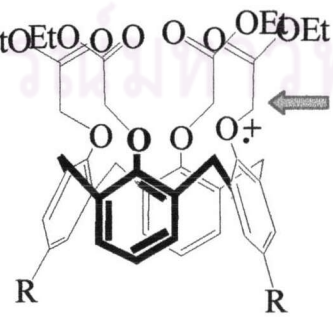

Figure 3.3.31 Show the oxidized oxygen atom of aryl ether unit

At various scan rates (shown in **Figure 3.3.32**), there was no oxidation peak appeared in the voltammograms. This implied that the characteristic of these electron transfer is an *EC* mechanism.[137] The deposition of the oxidized species may also occurred since not only the disappearance of reductive wave intensities but also the decrease of intensities of oxidation wave belonging to the ferrocenium unit. The species obtained from the oxidation of aryl ether unit were possibly adsorbed on the surface of the working electrode. (**Figure 3.3.34**)

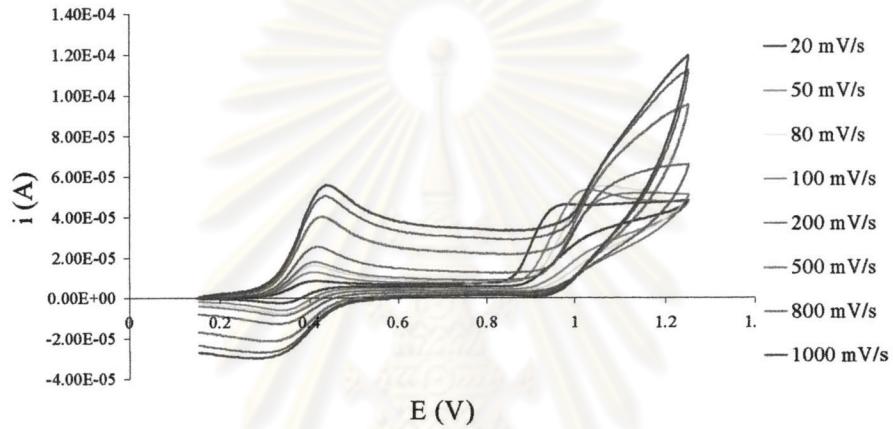

Figure 3.3.32 Cyclic voltammograms of **5a** at different scan rates

We focused our attention on the potential in the range of 0.15-0.55 V because we would like to study the effect of anion to the electron transfer process of the ferrocene unit. Titrations were carried out by addition of aliquots of tetrabutylammonium salts of benzoate, acetate, $H_2PO_4^-$ and Cl^- and followed by measurements at the scan rates of 50 mV/s. Addition of anion was varied from 0.2 to 4.0 equivalents. The feature of cyclic voltammograms of **5a** with benzoate was shown in **Figure 3.3.33 (a)**. Titrations of **5a**, **5b** and **5c** with caboxylate anion display the progressive appearance of a new wave at a less positive potential and a progressive disappearance of the initial wave. Titrations were also carried out in the square wave mode. It was found that not only the new wave gradually appears at less positive potential but also the initial wave decreases and disappears completely as shown in **Figure 3.3.33 (b)** and the K(+) and ΔE values shown in **Table 3.3.10**. The replacement of initial wave by the new one is complete after addition of excess anions (4.00 equivalents). Furthermore, the complexes of all ligands

and anions show irreversible electrochemical systems. Presumably, the Fc^+ unit enhanced binding with anionic species using the electrostatic interactions.

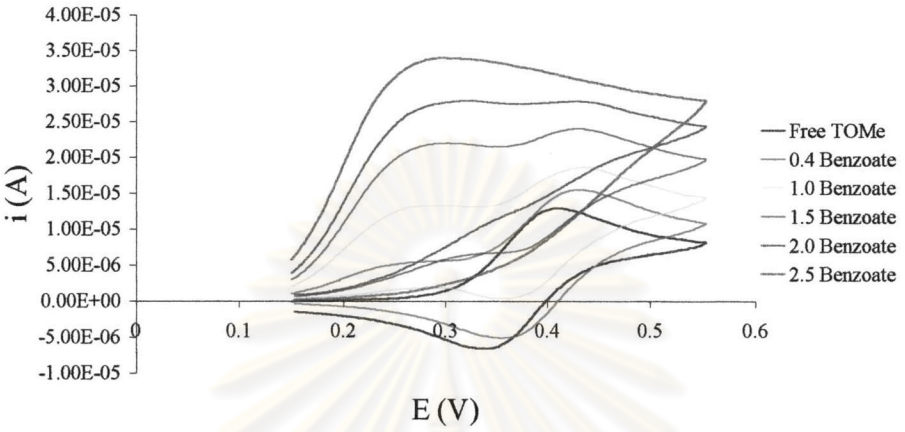

(a) Cyclic voltammograms titration with 0.1 M TBAPF in acetonitrile at 50 mV/s

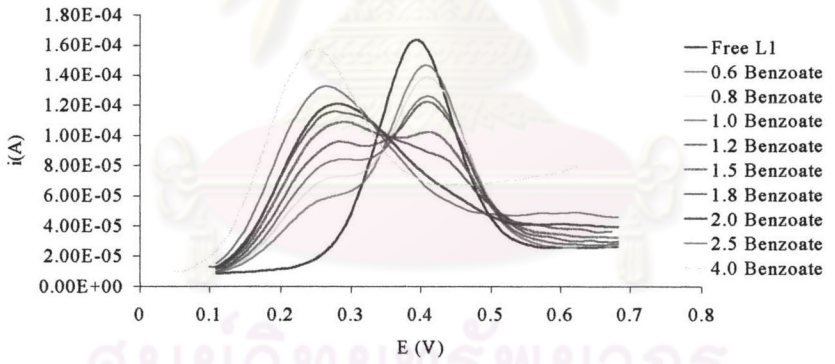

(b) Square wave titration at 50 mV/s and at frequency 60 Hz

Figure 3.3.33 Titration between **5a** and NBu_4PhCOO in acetonitrile with 0.1 M TBAPF

The ion-pairing associations are accompanied by adsorption phenomena according to the poor solubility of ion pair in solution. On the other hand, when an anion forms complex with amide ferrocenium unit, it probably blocks the electron released by the oxidation cycle. The result was observed by a loss of reversibility of Fc/Fc^+ redox wave. In contrast, cyclic voltammogram behaviors for Fc center of ligands and $H_2PO_4^-$ and Cl^- display small cathodic shift in Fc/Fc^+ redox potential (one wave behavior), indicating the

weak interaction of $H_2PO_4^-$ and Cl^- with ligands (**Figure 3.3.34** and **3.3.35**)

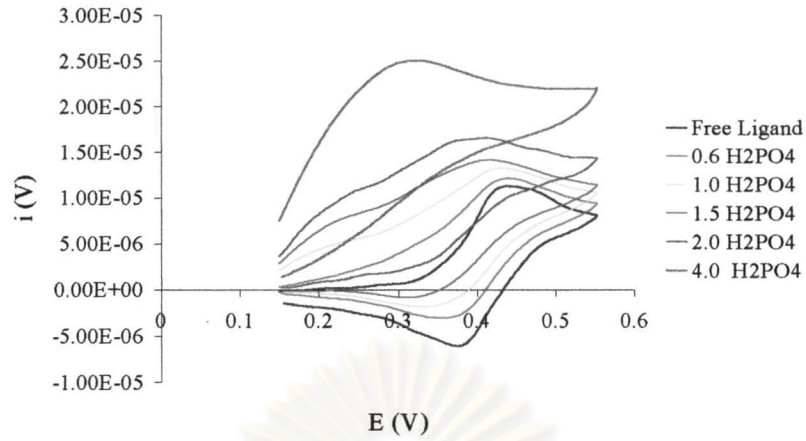

(a) Cyclic voltammogram titration at 50 mV/s.

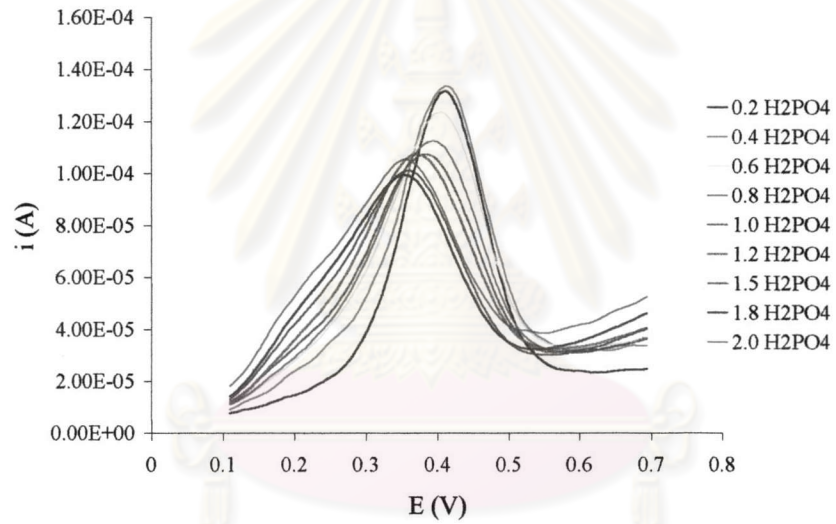

(b) Square wave titration at 50 mV/s and at 60 Hz.

Figure 3.3.34 Titration of **5b** and $NBu_4H_2PO_4$ in CH_3CN with 0.1 M TBAPF

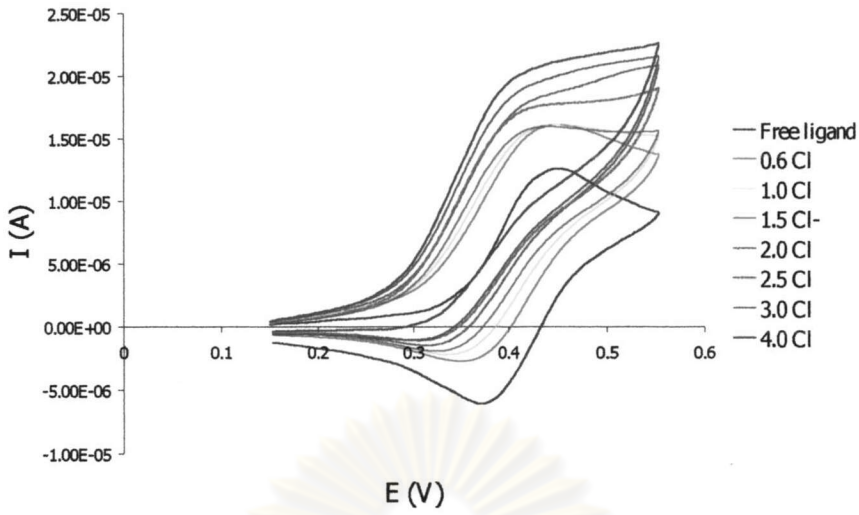

Figure 3.3.35 Titration of **5b** and NBu_4Cl in CH_3CN with 0.1 M TBAPF

Considerably, the cyclic voltammograms of complexes is conceptually similar to Astruc's works. In principle, Kaifer[141] studied the switching between binding states which can be classified broadly into two categories, *binary* and *incremental*. The binary case refers to the situation without the affinity between either cation or anion and the neutral ligand, but an interaction occurring under the redox-system. The incremental case refers to all situations observed by a finite binding between cation or anion and the neutral ligand and an interaction enhancement upon the redox ligand. The electrochemical properties of our works are classified into the incremental case because the incremental behavior is more suiltable for rapid interconversions of molecular structure due to kinetic availability of the bound species in both binding states exhibiting two waves upon addition of guest molecules. As the same rationalization, we can deduce the mechanism of electrochemical properties of complexes as shown in **Scheme 3.3.2**. [143-144]

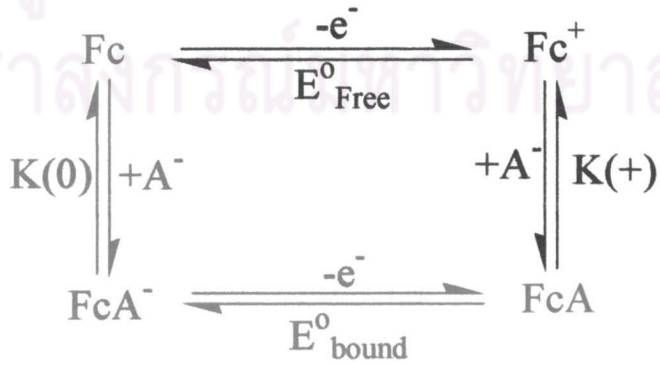

Scheme 3.3.2 The mechanism of electrochemical properties for complexes

The mechanism consists of four reactions in a square path, the total Gibbs free energy change (ΔG) in this cycle is thus zero. Importantly, the equilibrium is possibly approached via 2 routes, which cannot prove the exact machanism. The clock-wise route takes the pathway of oxidation of ferrocene unit to ferrocenium unit prior to bind with anionic species. Otherwise, the other route was described that the neutal ligands form complexes with anionic species and the Fe^{II} in complexes were oxidized to be Fe^{III} species. However, we assumed the equilibrium via a clock-wise route. The stability constant K of host/guest (1:1) complex is mathematically defined by equilibrium shown in **Scheme 3.3.2** where Fc and A^- represent the ferrocene unit and anions, respectively.

The total Gibbs free change energy.;

$$\Sigma\Delta G = \Delta G_{free} + \Delta G_{(+)} + \Delta G_{bound} + \Delta G_L = 0 \qquad (1)$$

By considering ΔG in term of thermodynamic energy: $\Delta G = RTlnK$ and in the case of thermodynamic potential in reaction expressed in $\Delta G = -nFE^{o}_{cell}$.

Thus, put ΔG parameter into the equation 1

$$-nF(E^{o}_{free}-E) - RTlnK_{(+)} + nF(E^{o}_{bound}-E) + RTlnK_{(L)} = 0 \qquad (2)$$

$$nF(E^{o}_{bound}-E^{o}_{free}) = RTlnK_{(+)} - RTlnK_{(L)} \qquad (3)$$

$$\frac{K_{(+)}}{K_{(L)}} = e^{[-nF(E^{\circ}bound-E^{\circ}free)/RT]}$$

$$K_{(+)} = K_{(L)}e^{[-nF(E^{\circ}bound-E^{\circ}free)/RT]} \qquad (4)$$

$K_{(+)}$ = association constant of anion with ferricinium

$K_{(L)}$ = association constant of anion with ferrocene

The ratio $K_{(+)}/K_{(L)}$ is a theoretically useful parameter because it allows not only the calculation of $K_{(+)}$ but also the evaluation of the effect of electron transfer on the complexation. In some cases, the relationship of $K_{(+)}/K_{(L)}$ is described in terms of the binding enhancement factor or BEF.[145] The stoichiometry of complexes is 1:1 between ligand and anion however, the binding enhancement factors were evaluated at 4.0 equivalents of anions which is the saturated point observed by no more potential shifted

further. As the former refined equation, the enhancement association constants of all complexes were shown in **Table 3.3.10**.

Table 3.10 The association constants of ligands in ferricinium forms with anions

Anions	5a			5b			5c		
	ΔE (V)	**$K_{(+)}$**	**BEF**	**ΔE (V)**	**$K_{(+)}$**	**BEF**	**ΔE (V)**	**$K_{(+)}$**	**BEF**
Acetate	0.08	18618	22.5	0.118	22470	99	0.130	189677	158
Benzoate	0.114	45755	84.7	0.136	27744	200	0.136	182631	200
$H_2PO_4^-$	a	-	-	0.084	2473	26.3	a	-	-
Cl^-	a	-	-	a	-		a	-	-

a; the uncertainties on ΔE values are estimated.

The stability constants measured by cyclic voltammetry give higher K values which are enhanced through the synergy between $X^{-}\cdots H$-N hydrogen bonding and electrostatic attraction in the oxidized forms. As mentioned above, the oxidized forms of ferrocene are in ferricinium form which prefers to bind anion species, especially for benzoate. The electrons on $-COO^-$ of benzoate are stabilized by aromatic ring resulting in the stable higher negative charge and the electron crowd of aromatic ring also enhanced the electrostatic interaction with ferricinium. According to the cyclic voltammograms of the titration between **5b** and $H_2PO_4^-$ and Cl^-, the initial peak shifts slightly to the lower positive potential. The results of $H_2PO_4^-$ and Cl^- measured by cyclic voltammetry are pertinent to those by ^{1}H-NMR titrations. It can be concluded that all ligands are unfavorable to bind with these anions.

Moreover, the cation binding ability studied by cyclic voltammetry are carried out by titrations between **5c** and $NaClO_4$ in acetonitrile with 0.1 M TBAPF. The potentials were measured in the range of 0.15 V to 1.3 V. As mentioned previously, the oxidation wave at 1.1 V belongs to aryl ether of ethyl ester groups.[146-147] This potential range is of interest in order to study changes upon the addition of cations. Cyclic voltammograms of titration experiments were depicted in **Figure 3.3.36**.

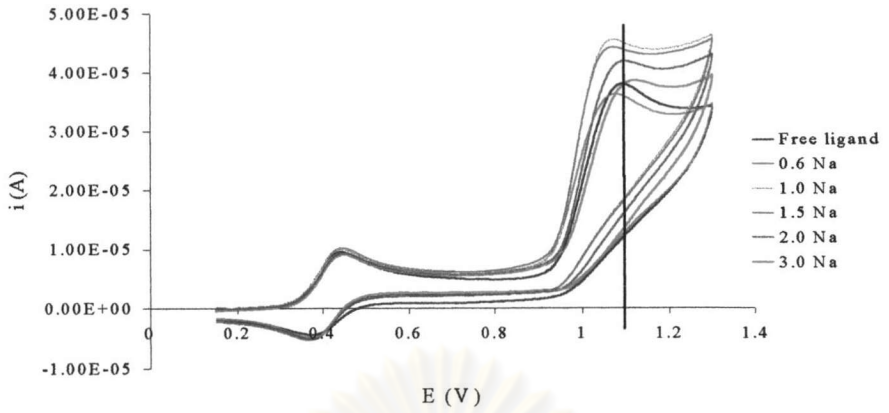

Figure 3.3.36 CV titrations of **5c** and $NaClO_4$ in acetonitrile using 0.1 M TBAPF as supporting electrolyte

The cyclic voltammograms can be separated into 2 sets depending upon the amount of added Na^+. In the first set, the cyclic voltammograms upon addition of $NaClO_4$ from 0 to 1.5 equivalents showed a slight shift of the oxidation wave to less oxidative potential. In the second set, the addition of Na^+ in the amount of 2.0 and 3.0 equivalents resulted in potential shift to higher oxidative potentials. However, we focused on the cyclic voltammogram of the free ligand with addition of excess cation (3.0 equivalent) in which the oxidative wave at 1.093 V shifted to the higher oxidative potential. (**Figure 3.3.37)** Additionally, the backward current belonging to ferrocene unit, increased significantly and caused the reduction of the i_{pa}/i_{pc} ratio as shown in **Table 3.3.11**.

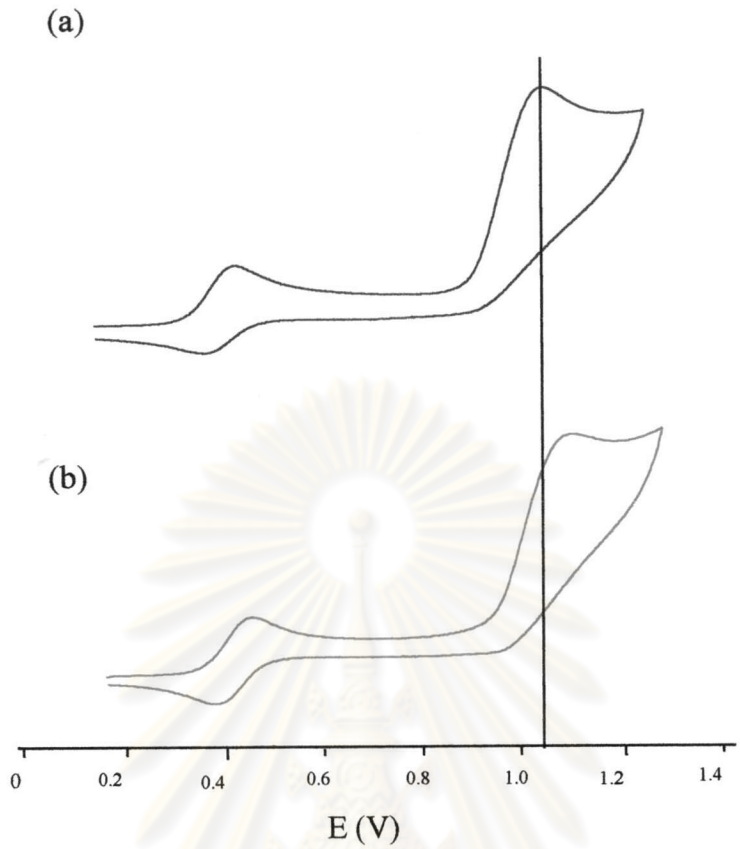

Figure 3.3.36 Cyclic votammograms of **5c** (a) and complex of **5c** with Na^+ (b) in acetonitril with 0.1 M TBAPF

Table 3.3.11 The i_{pa}/i_{pc} ratios of ferrocene couple upon the addition of $NaClO_4$

ligand: Na	i_{pa}/i_{pc}
1.0:0	2.005
1.0:0.6	1.445
1.0:1.0	1.372
1.0:1.5	1.319
1.0:2.0	1.267
1.0:3.0	1.159

According to the movement of the oxidation wave at 1.1 V to higher potential upon adding excess $NaClO_4$, it may imply that the aryl ether units of **5c** in the presence of $NaClO_4$ are oxidized harder than those of **5c** in the absence of $NaClO_4$ since the cation

binding at ethyl ester groups destabilize the aryl ether units in their oxidized forms. Additionally, the decrease of oxidatized species reduced the deposition on the surface of the electrode and resulted in the increase of the backward currents belonging to the ferricinium unit. From the results of cation titration by cyclic voltammetry, it supported the results from electrospary ionization mass spectroscopy that **5c** has ability to bind cation, even weak interactions. Unfortunately, the effects of cation towards anion recognition cannot be carried out by cyclic voltammetry because no changes upon addition anions in the presence of $NaClO_4$ took place obviously and the precipitate occurred during the addition of anions. We assumed that Na^+ bounded with ethyl ester group was removed and formed the precipitates.